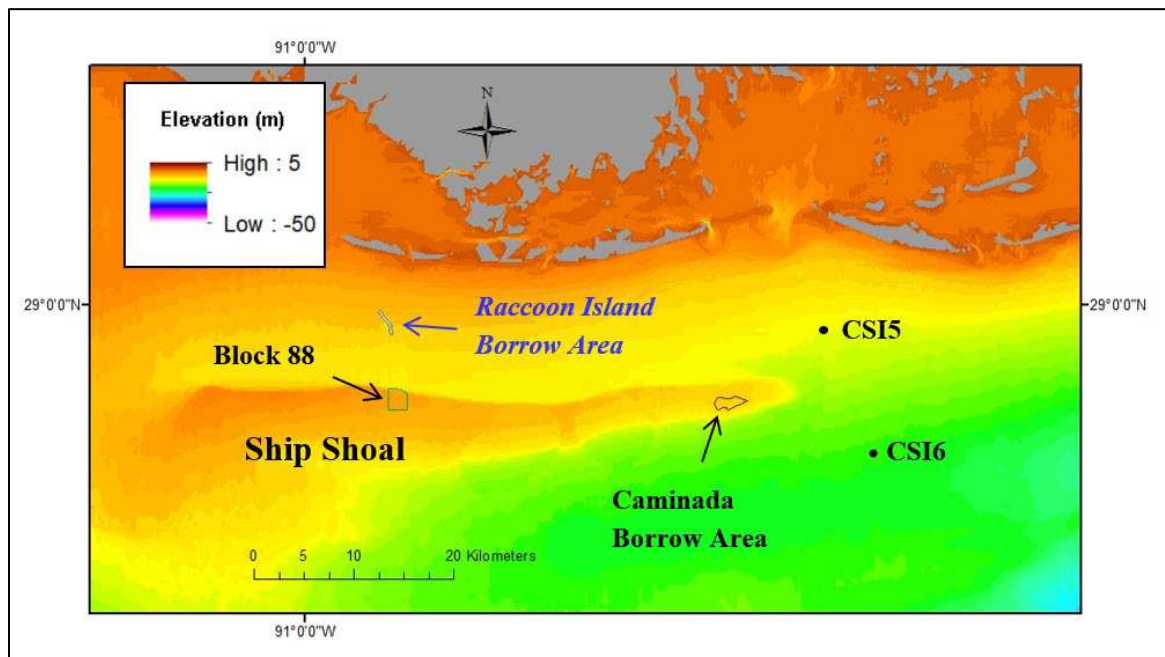


# Assessment of Ship Shoal Borrow Areas for Coastal Restoration of Louisiana Barrier Islands



US Department of the Interior  
Bureau of Ocean Energy Management  
Gulf of Mexico Regional Office  
New Orleans, LA



# Assessment of Ship Shoal Borrow Areas for Coastal Restoration of Louisiana Barrier Islands

May 2024

Authors:

Kehui Xu, Samuel J. Bentley, Chunyan Li, Carol Wilson, Haoran Liu, Grant Lopez, Kelli Moran,  
Zhenwei Wu, and Zehao Xue

Prepared under M16AC00018

by

Louisiana State University  
93 South Quad Drive  
Suite 1002  
Baton Rouge, LA 70803

**US Department of the Interior  
Bureau of Ocean Energy Management  
Gulf of Mexico Regional Office  
New Orleans, LA**



## DISCLAIMER

Study collaboration and funding were provided by the US Department of the Interior, Bureau of Ocean Energy Management (BOEM), Environmental Studies Program, Washington, DC, under Agreement Number M16AC00018 with Louisiana State University. This report has been technically reviewed by BOEM, and it has been approved for publication. The views and conclusions contained in this document are those of the authors and should not be interpreted as representing the opinions or policies of the US Government, nor does mention of trade names or commercial products constitute endorsement or recommendation for use.

## REPORT AVAILABILITY

Download a PDF file of this report at [https://espis.boem.gov/Final%20Reports/BOEM\\_2024-058.pdf](https://espis.boem.gov/Final%20Reports/BOEM_2024-058.pdf).

To search for other Environmental Studies Program ongoing and completed studies, visit <https://www.boem.gov/environment/environmental-studies/environmental-studies-information/>.

## CITATION

Xu K, Bentley S, Li C, Wilson C, Liu H, Lopez G, Moran K, Wu Z. 2024. Assessment of Ship Shoal Borrow Areas for coastal restoration of Louisiana barrier islands. New Orleans (LA): US Department of the Interior, Bureau of Ocean Energy Management. Obligation No.: M16AC00018. Report No.: BOEM 2024-058. 40 p.

## ABOUT THE COVER

Map showing the locations of two dredge pits at Caminada and Block 88 in Ship Shoal area, and Raccoon Island borrow area in northern Louisiana. Black dots are Louisiana State University WAVCIS (wave-current information system) stations at CSI5 and CSI6. The background color contours are bathymetry from ETOPO1 Global Relief Model<sup>1</sup>.

---

<sup>1</sup> See <https://www.ncei.noaa.gov/access/metadata/landing-page/bin/iso?id=gov.noaa.ngdc.mgg.dem:316>.

## Contents

List of Figures.....	v
List of Abbreviations and Acronyms.....	vi
1 Introduction .....	7
2 Objectives .....	10
3 Methods .....	11
3.1 Geophysical Data Acquisition.....	11
3.2 Submersible Vibracoring and Short Multicoring .....	11
3.3 Hydrodynamic Data Acquisition and Analyses .....	11
3.4 Laboratory Work .....	11
4 Results .....	12
4.1 Block 88 Geophysical Results .....	12
4.2 Block 88 Core Results .....	16
4.3 Caminada Geophysical Results .....	20
4.4 Caminada Core Results.....	25
4.5 Caminada ADCP Results .....	28
5 Discussion and Conclusions .....	31
5.1 Sediment Transport Processes .....	31
5.2 Conceptual Pit Morphology Model.....	32
5.3 Recommendations and Future Work.....	33

## List of Figures

Figure 1. Conceptual model.....	7
Figure 2. Study area.....	8
Figure 3. Block 88 sidescan sonar mosaic. ....	13
Figure 4. Block 88 subbottom data. ....	13
Figure 5. Block 88 bathymetry data. ....	15
Figure 6. Block 88 slope.....	16
Figure 7. Block 88 grain size distribution. ....	17
Figure 8. Block 88 grain size color plot. ....	18
Figure 9. Block 88's <sup>7</sup> Be activity plot.....	19
Figure 10. Block 88 X-ray images.....	20
Figure 11. Caminada bathymetry map.....	21
Figure 12. Caminada sidescan map. ....	22
Figure 13. Caminada slope map.....	23
Figure 14. Caminada bathymetry and sediment comparison. ....	24
Figure 15. Caminada grain size color plot. ....	26
Figure 16. Caminada x-ray images.....	27
Figure 17. Caminada Beryllium-7 activity. ....	28
Figure 18. Caminada ADCP velocity. ....	30
Figure 19. Conceptual pit morphology model. ....	33

## List of Abbreviations and Acronyms

Short form	Long form
ADCP	acoustic doppler current profiler
BAMM	Borrow Area Management and Monitoring program
BOEM	Bureau of Ocean Energy Management
CDP	Caminada dredge pit
CPRA	Coastal Protection and Restoration Authority of Louisiana
DoD	difference of depth
EPA	US Environmental Protection Agency
Gulf	Gulf of Mexico
LOI	loss-on-ignition
LSU	Louisiana State University
MC	multicorer
MCDP	mud capped dredge pit
MMP	Marine Minerals Program
NTU	nephelometric turbidity unit
OCS	Outer Continental Shelf
SP	Sandy Point dredge pit
SDDP	sandy dredge disposal pits
SSBA	Ship Shoal borrow area
SSC	suspended sediment concentration
USGS	US Geological Survey

# 1 Introduction

Barrier islands are coastal landforms made up of sandy sediments that are separated from the mainland by estuaries or lagoons. These islands act as natural buffers, protecting the mainland coast and inland wetlands from meteorological and marine forces and helping to regulate conditions within the estuaries (Nittrouer et al., 2008). In Louisiana, a significant part of the effort to manage coastal land loss involves restoring degraded barrier shorelines by dredging sand resources from borrow sites and delivering them to coastal sedimentary environments. However, dredging activities at these borrow sites can have substantial impacts on the sea floor and nearby environments, raising concerns among various experts including oceanographers, engineers, benthic ecologists, archeologists, environmental scientists, and decision-makers. It is noted that approximately 90% of the sediment load carried by the Mississippi and Atchafalaya Rivers is suspended mud, with only about 10% being sand (Nittrouer et al., 2008). Therefore, understanding the spatial and temporal variations in the formation of limited sand resources along the Mississippi River Deltaic Plain is critical for the success of many dredge projects. Penland et al. (1989) proposed a conceptual model illustrating the formation of sediment deposits under both regressive and transgressive environments (Figure 1). According to this model, after river abandonment, prograded deltaic headlands are reworked by marine processes, leading to transgression and their transformation into ebb tidal deltas and sandy submarine shoals.

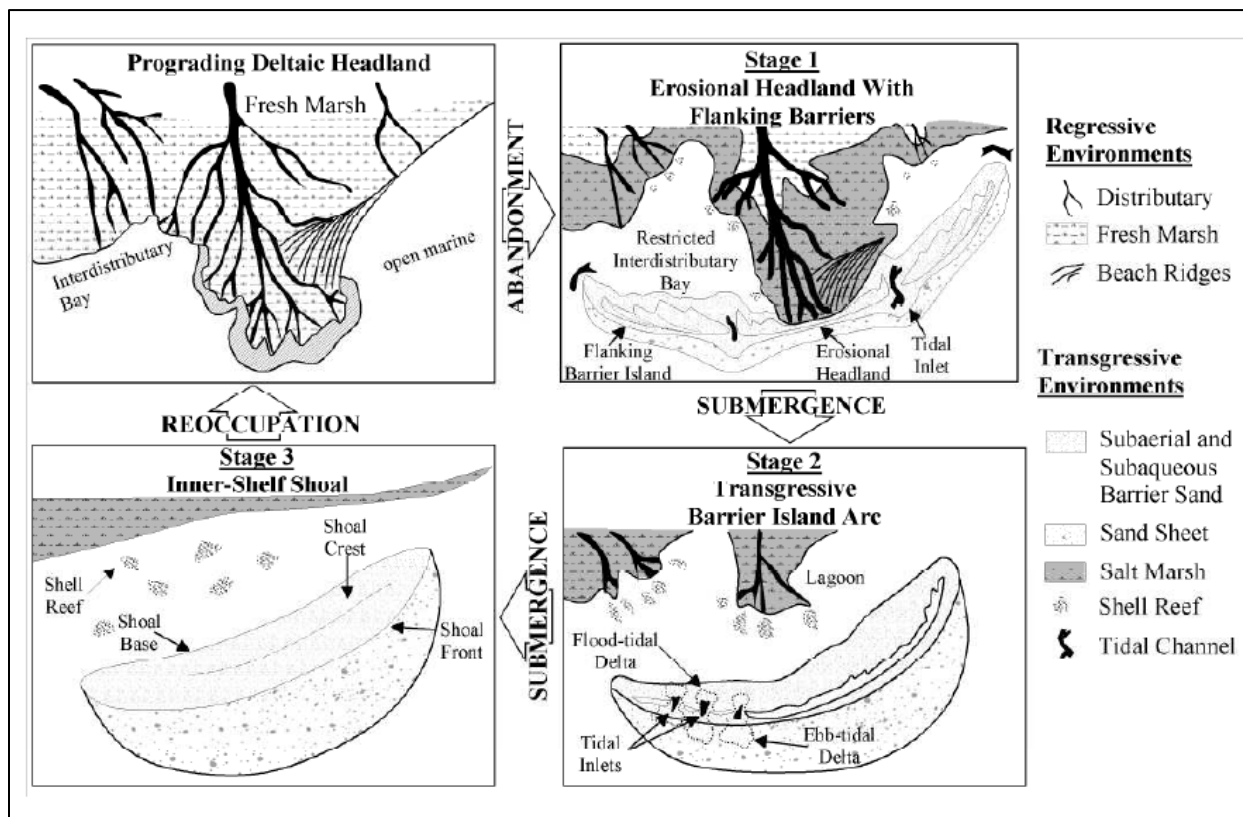


**Figure 1. Conceptual model**

A conceptual model showing the formation of transgressive and regressive depositional systems along the Louisiana coastal zone (Penland et al., 1989).

The Louisiana shelf is home to significant sand resources, primarily in the form of submarine sandy shoals like Ship Shoal, Tiger and Trinity Shoals, and Sabine Bank. These shoals are influenced by various factors including wind-driven currents, storm waves, tides, and the dynamic dispersal systems of the Atchafalaya and Mississippi Rivers. They also serve as important habitats for various marine species, providing grounds for spawning, hatching, and foraging (Munnely, 2016). Over the past few decades, many oil and gas pipelines have been installed on these sandy shoals, which need to remain buried as the seafloor evolves after it is dredged. The Marine Minerals Program (MMP) at the Bureau of Ocean Energy Management (BOEM) and the State of Louisiana are interested in finding ways to efficiently utilize these sand resources while minimizing impacts on the pipelines, sensitive seafloor habitats, and potential cultural resources (Nairn et al., 2005; Research Planning et al., 2004).

During recent years, the eastern end of Ship Shoal has been used as a borrow area for Caminada Headland Beach and Dune Restoration Project Increments 1 and 2 (Figure 2). This project excavated approximately 10 million cubic yards of sand. In addition, Ship Shoal Area Block 88 (in the middle of Ship Shoal, Figure 2) was used as a borrow area where approximately 13.4 million cubic yards of sand was excavated to construct the Caillou Lake Headlands (Whiskey Island) Beach and Marsh Restoration Project in 2015.

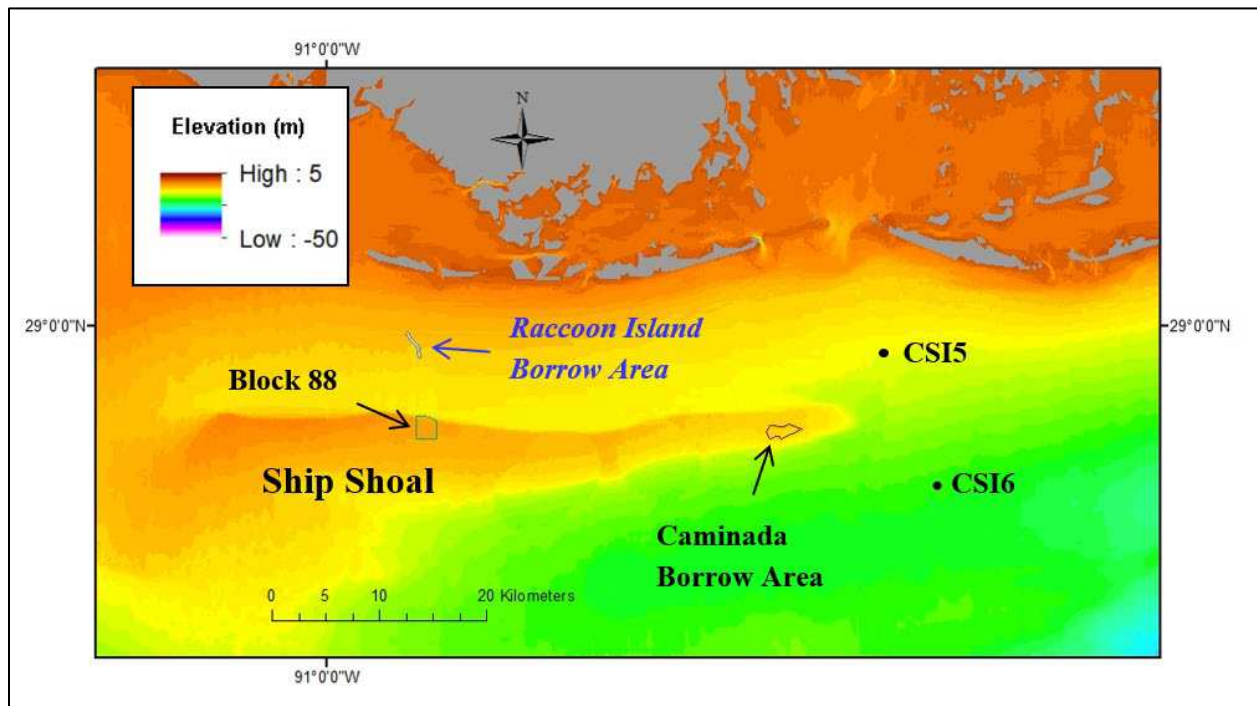


**Figure 2. Study area.**

Map showing the locations of the Caminada and Block 88 in Ship Shoal borrow areas. CSI5 and CSI6 are LSU WAVE-Current Information System (WAVCIS) stations and Raccoon Island is a mud-capped dredge pit. The background color contours are bathymetry from ETOPO1 Global Relief Model (<https://www.ncei.noaa.gov/access/metadata/landing-page/bin/iso?id=gov.noaa.ngdc.mgg.dem:316>).

The study areas of this project are Caminada and Block 88 borrow areas in Ship Shoal (Figure 2). The Louisiana Coastal Protection and Restoration Authority (CPRA) has implemented their Borrow Area Managing and Monitoring (BAMM) program that has been monitoring physical changes and impacts to water quality at borrow areas within state waters and some Outer Continental Shelf (OCS) sites. Our study complements BAMM and other programs focused on long term sediment management and helps understand the impacts of mining sediment for coastal restoration and improve sand resource management efforts.

Ship Shoal is one of the largest offshore sand resources along the northern Gulf of Mexico, containing 1.22 billion m<sup>3</sup> of fine sand (Stone et al., 2009; Figure 2). The shoal is approximately 50 km long and 5-12 km wide. Water depth ranges from 7 to 9 m on the eastern side of the shoal to approximately 3 m on the western side. Over 2,000 km of high-resolution seismic data and 50 offshore vibracore borings have been collected by the Louisiana Geological Survey, U.S. Geological Survey (USGS), CPRA and BOEM in the past. Stone et al. (2000, 2009) conducted detailed studies of hydrodynamics and sediment dynamics using combined empirical measurements, modeling, and some biological studies of benthic habitats and nekton species in this area. Stone et al. (2009) reported that the combination of spring flood discharge from the Atchafalaya River and the passing of post-frontal phases of cold front meteorological events can lead to sediment transport to Ship Shoal. They also hypothesized that occasional sediment plume shifts from the Atchafalaya Bay to the southeast may result in the accumulation of a thin fluid mud layer on patchy portions of the shoal with a maximum thickness of about 2-4 cm. However, tens of vibracores collected extensively in the Ship Shoal area all show clean and high-quality beach-compatible sand with essentially no mud preserved. These findings indicate that fluid mud may temporarily blanket the Shoal but is later transported elsewhere to deeper water. However, this could be a mechanism for mud infilling at excavations on the shoal, which is a consequence of dredge projects.

Over the past twenty years, extensive studies have been conducted on both the Caminada and Block 88 borrow areas. Initially, Kulp et al. (2001) identified the Caminada borrow areas as suitable candidates for restoration and other projects, particularly those situated on the far eastern portion of Isle Dernieres and the Terrebonne/Barataria Basin. Subsequently, more comprehensive geophysical and archaeological investigations were carried out in the Caminada borrow area in 2003. These efforts were part of the feasibility study of the Louisiana Coastal Area Barataria Basin Barrier Shoreline Restoration project (Breland et al., 2015). During the design phase, Caminada Increment I was planned, permitted, and executed under the Coastal Impact Assistance Program. Following this, Caminada Increment II was designed and finished, funded by settlement funds managed by the National Fish and Wildlife Foundation (Breland et al., 2015).

Block 88 on Ship Shoal has been identified as a borrow area for several nearby barrier island restoration projects. The Block 88 seabed is sandy with a median grain size of 0.2 mm (Nairn et al., 2005). Its proposed borrow area is approximately 2.5 × 2.5 km. Block 88 was proposed to be used in the Caillou Lake Headlands Restoration Project which was originally recommended through Terrebonne Basin Barrier Shoreline Feasibility Study as the first component for construction of the National Ecosystem Restoration Plan. A conveyance corridor was used to pump sediment slurry from Block 88 to Caillou Lake Headlands and nearby areas.

Nairn et al. (2005) applied a 1-D analytical model, originally developed by Ribberink et al. (2005), to study the evolution of a sandy pit in Block 88. They found that bed load, rather than suspended load, is the dominant form of sediment transport, potentially even exceeding the suspended load in magnitude. In Block 88, changes in the pit slope position are primarily driven by bed load, while infilling is influenced by both bed load and suspended load. This close coupling between infilling and pit slope change was noted. This study also revealed that Block 88's pit can fill up relatively quickly, typically within 3-5 years. The migration of the pit occurs towards the west and north; westward migration is attributed to the net residual current in that direction, while northward migration is linked to the process causing Ship Shoal to migrate shoreward (Nairn et al., 2005). The rate of pit migration was determined using the approach by Ribberink et al. (2005) and is highly sensitive to various parameters, including the speed of the residual current and other physical oceanographic factors.

Based on their comprehensive studies, Nairn et al. (2005) proposed a conceptual diagram of pit infilling and pit margin erosion processes. As flow leaves the pit and water depth is reduced, the flow speed increases to match the ambient flow speed in the absence of the pit. The sediment load capacity of the

flow at the outgoing edge is like the load capacity at the incoming edge based on the conservation of water mass. However, the suspended sediment concentration at the outgoing edge is less than capacity once the flow accelerates to ambient flow speed due to deposition in the pit. This results in bed erosion beyond the outgoing edge to restore sediment concentration to an equilibrium level. Finally, Nairn et al. (2005) recommended a minimum buffer distance of 50 to 100 m for pipelines and other submerged oil and gas seabed infrastructure. The lower limit would be appropriate where the location of the nearby infrastructure is accurately surveyed prior to final design of the dredge pit. For above water structures such as platforms, a minimum recommended buffer distance would be 500 m based primarily on navigational considerations.

Modifications to seafloor topography resulting from dredging sediment resources have the potential to impact nearby oil and gas infrastructure and other resources located close to dredge pits. While the direct effects of dredging are well understood, our knowledge of the long-term evolution of borrow pit geometry is limited. BOEM allocated funding to enhance our understanding of how dredge pits evolve and their potential impacts on adjacent infrastructure and resources (Nairn et al., 2005, 2007; Stone et al., 2009). However, there is a lack of site-specific data necessary for accurate predictions and empirical measurements to validate predictive models in sand-dominated dredge pits. Our study aims to address these gaps by building on BOEM's efforts. We focus on filling data gaps, validating predictive models, and assessing the effectiveness of mitigation measures applied to existing dredge pits to safeguard resources and infrastructure. The outcomes of this project can enhance models that rely on empirical data for predictions and provide essential information for National Environmental Policy Act (NEPA) analyses and related consultations.

Xu et al. (2016) reported up to about 0.5–1 m/year of sediment deposition in a mud-capped Raccoon Island dredge pit which is 6 km north of Ship Shoal (Figure 2). This pit is much narrower and deeper than the Caminada or Block 88 borrow area. If the Caminada and Ship Shoal Block 88 borrow areas can trap a significant amount of high-quality sand from slope adjustment/sediment redistribution of Ship Shoal, these borrow sites might be reused for future restoration projects. This would significantly benefit coastal Louisiana restoration. On the other hand, if a significant amount of mud is trapped in the pit, or the mud-sand lamination is preserved, the change from sandy to muddy (or even mixed) substrate on Ship Shoal may influence the activities of fish species and benthic communities and reduce quality of fill for barrier island use.

## 2 Objectives

The main objectives of this study are to:

- 1) Quantify borrow area geomorphic evolution (e.g., wall slope geometry, infilling rate, edge migration, etc.) by collecting new physical oceanographic, geological and geophysical data in two Ship Shoal Borrow Areas (Caminada and Block 88);
- 2) Validate the model of Nairn et al. (2005) with newly collected data;
- 3) Identify the type and quality of infilling sediment and quantify sediment accumulation rates;
- 4) Assess the effectiveness of existing mitigations;
- 5) Provide recommendations for pit monitoring protocols (e.g., assigned setback buffer zone) as well as suggest mitigations based on measurements;
- 6) Provide recommendations for future mineral management and dredging projects.
- 7) Develop a conceptual geomorphic evolutionary model to improve our understanding of sediment transport and infilling processes in Ship Shoal Borrow Areas.

### 3 Methods

In Caminada dredge pit, two post-dredging surveys and corings were in July 2017 and August 2018, respectively. In Block 88 pit, the research was pushed back due to delays on dredging, but field activities were in June 2019 and September 2020, respectively. Our field data collection methods included: 1) hydrodynamic observation and hydrographic data collection using a bottom-mounted ADCP (Acoustic Doppler Current Profiler); 2) shallow geophysical surveying using high-resolution swath bathymetry, sidescan sonar, and seismic sub-bottom profiler; and 3) collection of vibracores and multicores sampled for texture and radionuclide analyses of cored sediment. Below are brief methods used in this project.

#### 3.1 Geophysical Data Acquisition

An Edgetech 4600 swath bathymetry and sidescan sonar system was used to collect data with a swath width up to 8 times the water depth. The swath sonar frequency was 540 kHz, and the depth range below the transducer was ~50m. The 4600-system produced real-time high-resolution three-dimensional maps of the seafloor while providing co-registered simultaneous sidescan and bathymetric data. Seafloor features, such as pit edges, failure scarps, and bedforms as small as 10-20 cm could be imaged. The Edgetech 2000 DSS combined sidescan sonar & sub-bottom profiler system was used to collect CHIRP seismic profiles using a range of frequency of 2–16 kHz and sidescan data using simultaneous frequencies at both 300 and 600 kHz. The 2000 DSS system's sub-bottom profiles could reveal erosional and depositional structure with a vertical resolution of 6–10cm and a 60 m penetration depth over a muddy sea floor. In addition, an Edgetech 0512i subbottom profiler was used to achieve deeper subbottom penetration, but at coarser vertical resolution. More detailed methods can be found in Moran et al. (2022).

#### 3.2 Submersible Vibracoring and Short Multicoring

Based on the evaluation of geophysical data, core samples were collected to target specific features of interest. Two kinds of coring devices were used: a submersible vibracorer and a multicorer. The submersible vibracorer with electric motor was used to collect cores up to about 3–5 m long although the penetration operation into the sandy environment at Ship Shoal with energetic ambient currents proved to be challenging. An Ocean Instruments 4-tube multi-corer was used to collect cores up to 0.5 m long which preserve the water-sediment interface well. More detailed methods can be found in Xue et al. (2022).

#### 3.3 Hydrodynamic Data Acquisition and Analyses

The vessel-based surveys were planned with an objective of resolving spatial structures of the flow field in three dimensions around the dredged pit. A Teledyne RDI 600 kHz ADCP mounted on one side of the *R/V Coastal Profiler* was used to measure vertical profiles of the three-dimensional velocity vectors ( $u$ ,  $v$ , and  $w$ , or the east, north, and vertical components of velocity) at roughly half meter vertical intervals and recorded every second. The measurements took place as the research vessel moved along planned transects for bathymetry and seismic surveys that covered the sampling area.

#### 3.4 Laboratory Work

Our laboratory analyses included: laser grain size and loss-on-ignition organic matter; radioisotope geochronological analyses, multi-sensor logging for bulk density using a Geotek Multi Sensor Core Logger, and digital X-radiography of cores to study sediment layering. More detailed methods can be found in Xue et al. (2022), Moran et al. (2022), and Liu et al. (2022).

## 4 Results

The results are divided and summarized into five sub-sections: Block 88 geophysical, Block 88 Core, Caminada Geophysical, Caminada Core, and ADCP results. Over the past several years, the following five journal articles have been published as part of this BOEM study. For more detailed analyses and results, please refer to the following publications:

Moran et al. (2022)

Liu et al. (2022)

Xue et al. (2022)

Liu et al. (2020)

Liu et al. (2019)

### 4.1 Block 88 Geophysical Results

Block 88 geophysical results were published in Moran et al. (2022). Sidescan mosaics were generated from data collected in 2019 and 2020 and confirmed with surface sediment samples collected between the sidescan surveys (Figure 3). The mosaic maps indicate that the Block 88 dredge pit is slowly infilling with low reflectivity sediment; mostly clays and silts. Initial sediment infilling took place along the northwestern and central region of the pit, a region of topographic depressions, but over time, the muddy sediments expanded into ambient areas in the pit bottom. Beryllium-7 ( $^7\text{Be}$ ) data show that 10-12 cm of river-derived material was delivered to the Block 88 pit within a 6-month period before coring in August 2020. The pattern of  $^7\text{Be}$  with depth does not display typical exponential decay, but more of a vertical stepwise pattern, which suggests that either the sediment delivery was not constant but punctuated, or extreme bioturbation occurred in the cores. Despite these limitations, accumulation of 10 to 12 cm of  $^7\text{Be}$ -tagged sediment over six months implies a sedimentation rate of 0.2 to 0.25 m yr<sup>-1</sup>. Analysis of the 2020 sidescan data displays several bottleneck shaped slides in the northeast corner of the pit following the contour line of the pit wall. Subbottom profiles show an area of signal attenuation possibly associated with biogenic gas in the sediments as well as the collapse of the southern pit wall (Figure 4).

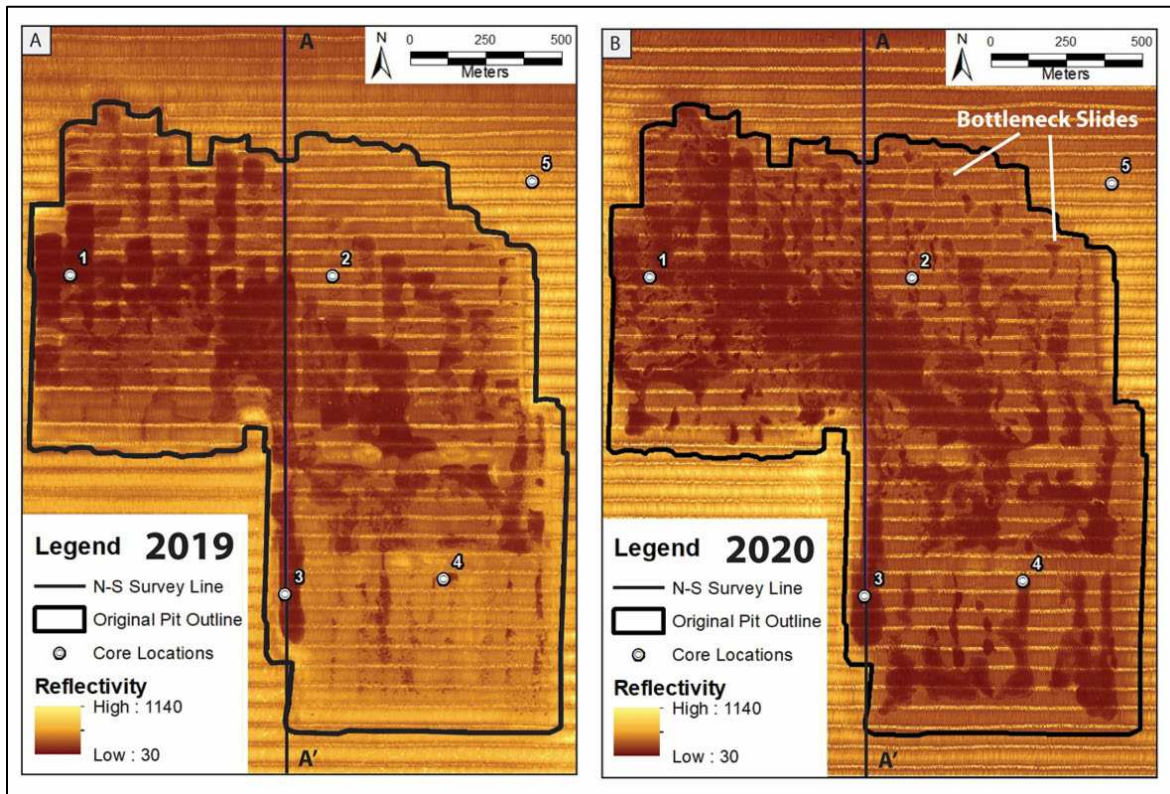


**Figure 3. Block 88 sidescan sonar mosaic.**

Sidescan sonar mosaic generated from the data collected in 2019 and 2020 at Block 88 dredge pit using an Edgetech 4600 system (co-registered swath bathymetry and sidescan sonar). The horizontal striping is an artifact of survey scanning. Dark brown areas indicate lower reflectivity and yellow areas indicate high reflectivity. The black line indicates the outline of the initial dredge pit as interpreted from the steepest slope of the original 2018 bathymetric survey (from Moran et al., 2022).

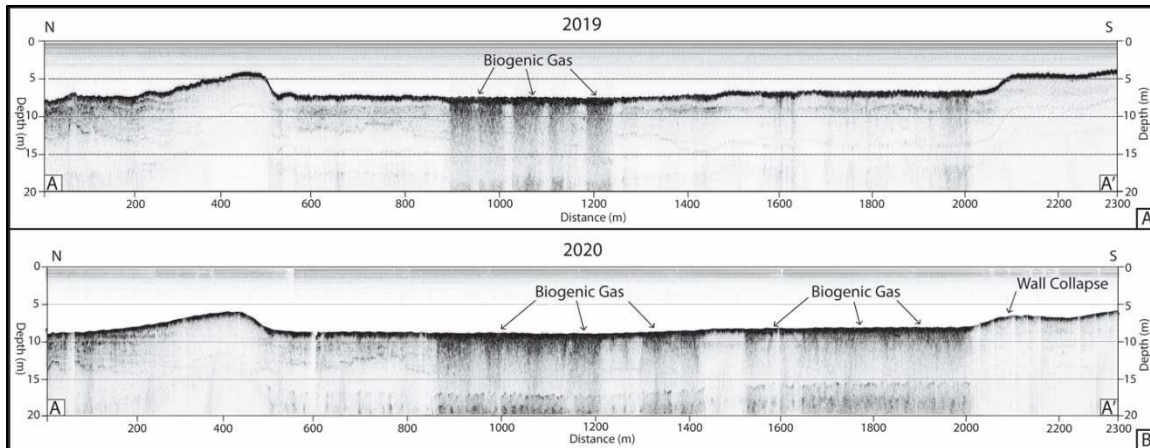


**Figure 4. Block 88 subbottom data.**

Subbottom data collected using an Edgetech 2000-DSS system (combined sonar and subbottom profiling). Both lines are the same North-South trending survey line collected along Line A-A' through the middle of Block 88 one year apart. See Figure 3 for location of Line A-A' (from Moran et al., 2022).

Bathymetric surveys show the Block 88 dredge pit is relatively stable, showing comparatively small pit wall migration between 2018, 2019 and 2020 (Figure 5). The 2020 data show depressions in the southwest portion of the pit, ranging from 25 to 90 m in width and 0.2 to 0.4 m in depth (Figure 5C), that are not present in the previous year's surveys (Figure 5). Difference of depth (DoD) maps indicate that there are areas of sediment deposition along the southern and eastern pit walls (Figure 5). Calculations using ESRI's ArcMap software reveal that the eastern pit wall alone has accumulated  $\sim 102,500 \text{ m}^3$  of sediment, which is equivalent to  $\sim 0.15$  million tons since the dredging completion of Block 88. The northern and western pit wall edges are hotspots for vertical erosion or pit wall collapse with areas of up to 2.5 m of vertical erosion and  $\sim 30$  m of horizontal wall migration (Figure 5).

Slope maps generated from the bathymetric surfaces collected in 2018, 2019, and 2020 show rapid smoothing of the pit bottom and a decline in averaged pit wall slope from  $\sim 10^\circ$  in 2018 to  $\sim 6^\circ$  in 2020 (Figure 6). At the time of the 2020 survey, the southernmost pit wall had largely collapsed, and the original topography of the pit is smoothed to  $< 5^\circ$  (Figure 6). The 2020 bathymetry and slope map data also display the outlines of depressions and slump features as well as the outward horizontal migration of the northwest pit wall  $\sim 30$  m. Based on the comparison of bathymetric profiles, overall infilling of the pit bottom at Block 88 between 2018 and 2020 is small with the middle of the pit accumulating less than 1 m over the three-year study (Figure 7). Assuming the minimum ( $0.2 \text{ m yr}^{-1}$ ) and maximum ( $0.25 \text{ m yr}^{-1}$ ) infilling rate indicated by the  $^7\text{Be}$  data, the volume of sediments accumulated at Block 88 would be between  $\sim 438,000$  and  $\sim 547,000 \text{ m}^3$ , respectively.

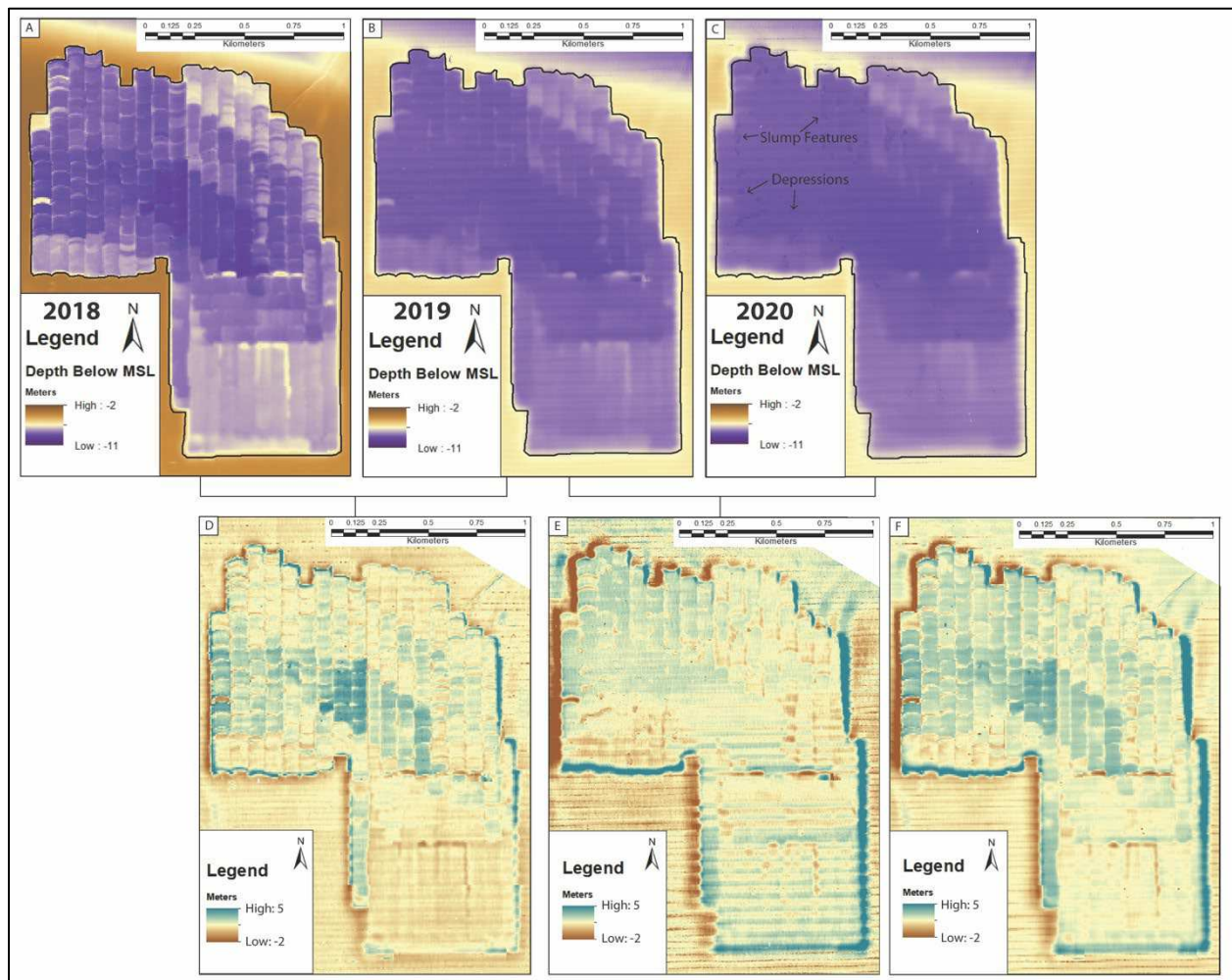


**Figure 5. Block 88 bathymetry data.**

Bathymetric surveys for 2018, 2019, and 2020 (panels A, B, and C, respectively). Panels D, E and F display Difference of Depth (DoD) maps between survey years: Panel D is between 2018 and 2019, Panel E is between 2019 and 2020, and Panel F is Total Difference of Depth indicating a total change since dredging between 2018 and 2020. Positive values indicate areas of infilling while negative values indicate areas of erosion. The total DoD map indicates that the pit has generally filled with the largest areas of sedimentation (~2.5 m) occurring along the eastern and southern pit wall edges. It also indicates that the largest area of erosion (up to 2.5 m of vertical erosion) occurred along the western edge and generally indicates minor pit migration to the WNW (from Moran et al., 2022).

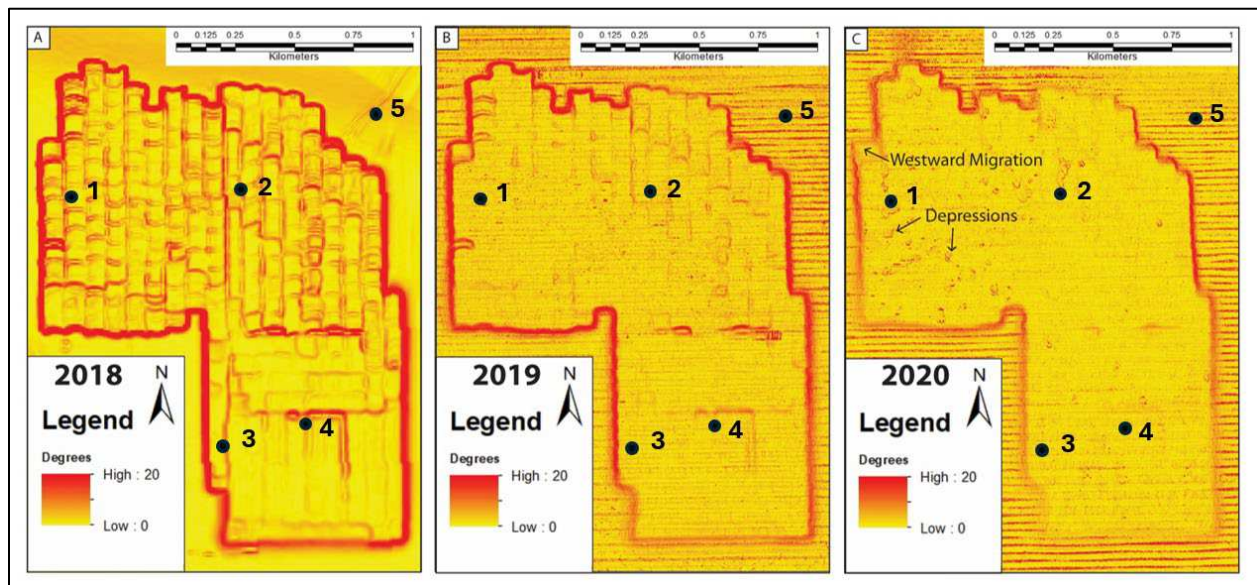


**Figure 6. Block 88 slope.**

Slope maps generated using the bathymetry collected immediately following dredging in 2018 and during the 2019 and 2020 seismic surveys. Reds are areas of steep slope and yellows are gentle slopes. The pit bottom of Block 88 smooths from 2018 to 2020 (also shown in Figure 7) and there is minimal topographical change in pit bottom in the 2020 data. The 2020 data also show that the parts of the northern and all the southern pit wall have collapsed indicated by the low slope angle. The 2020 data also appear to show migration of the northwest pit wall ~ 30 m to the west as well as the development of depressions in the southwest portion of the pit between the 2019 and 2020 surveys (from Moran et al., 2022).

## 4.2 Block 88 Core Results

Five cores were collected in Block 88 pit in the year 2020 (Figure 3). The core names are BL20-1 through BL20-5. Cores BL20-1, 2, and 3 showed 90-95% of the total infill was silt to clay grain sizes (Figure 7). Cores BL20-4 and 5 taken outside of Block 88 showed 60-100% of the total infill was very fine to medium sand (Figure 7). Core BL20-1 average infill grain size is 5-40  $\mu\text{m}$ , with thin laminations of coarse silt to fine sand. BL20-1 has one package of 70-200  $\mu\text{m}$ , very fine to fine sand, at a depth of 21.5–24.5 cm. Core BL20-3 showed an infill of slightly coarser grained sediment than BL20-1, with an average range from 5  $\mu\text{m}$  to 90  $\mu\text{m}$ . This core had bimodal grainsize peaks ranging from 20-200  $\mu\text{m}$  at 8–19 cm depth. BL20-3 had massive bedding of very fine to fine sand ranging from 90-200  $\mu\text{m}$  at 26 to 32cm. Both BL20-1 and BL20-3 are capped with a massive bed of 1-30  $\mu\text{m}$  clay to medium silt, with both displaying a fining upward sequence (Figure 8). Core BL20-3 in contrast has an abrupt shift from 40–200  $\mu\text{m}$  to 1-30  $\mu\text{m}$  at ~7.5 cm, after the bimodal sequences (Figure 8). The Ocean Instruments MC 400 Multicore device had difficulty collecting cores at BL20-2's pit location, similar issues were observed when extracting BL20-4 and BL20-5, leading to failure in capturing a full core profile (~50 cm). From the bottom of BL20-2 up to 8 cm there is predominantly 140-160  $\mu\text{m}$  fine sand material, while the upper 6 cm of core is predominantly 2–10  $\mu\text{m}$  clay to fine silt material (Figure 8). BL20-2 has finer grained material cap than is present on BL20-1 and BL20-3. Cores BL20-4 and 5 taken outside the pit are predominantly sand with BL20-5 being 100% composed of a >90  $\mu\text{m}$  very fine and fine sand. Core BL20-4 is also predominantly sand with 60% ranging from 63-250  $\mu\text{m}$ , very fine to medium sand, with the remainder 40% ranging from 0.5-63  $\mu\text{m}$ , from clay to coarse silt.

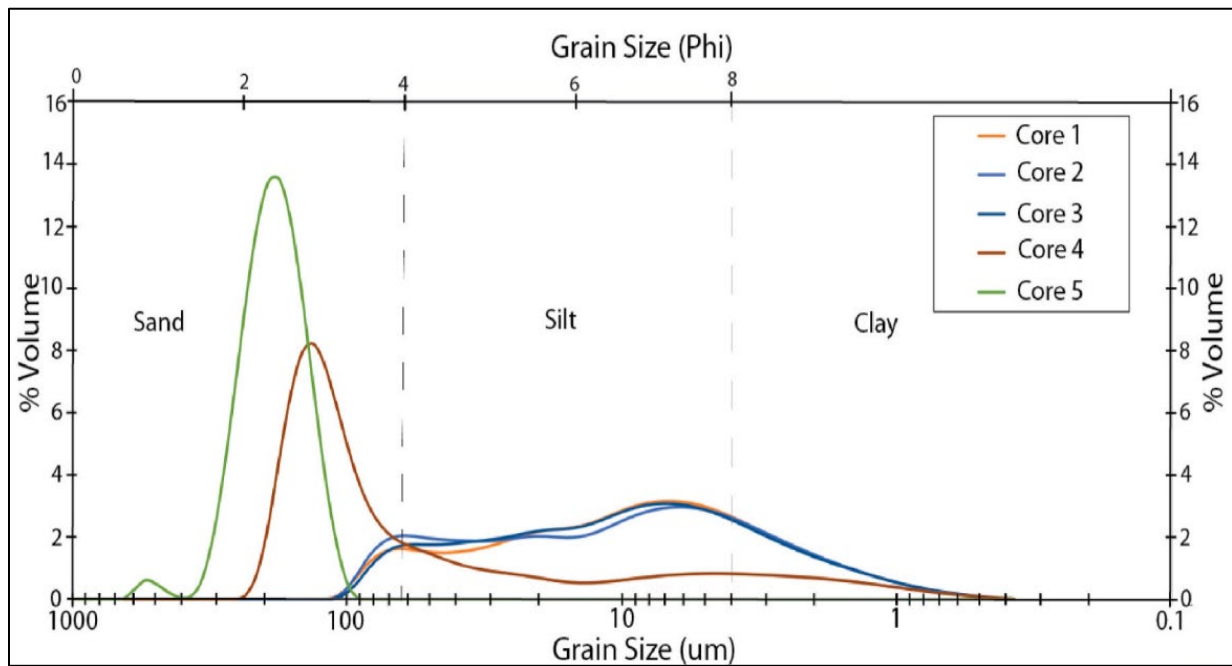


**Figure 7. Block 88 grain size distribution.**

Grain analysis showed the top 2 cm of sediment composition, cores within the pit ((Cores 1,2,3) were composed mostly of finer grained silty material, while those taken outside the pit (Cores 4/5) were of similar sandy make up to Ship Shoal (from Moran et al., 2022)

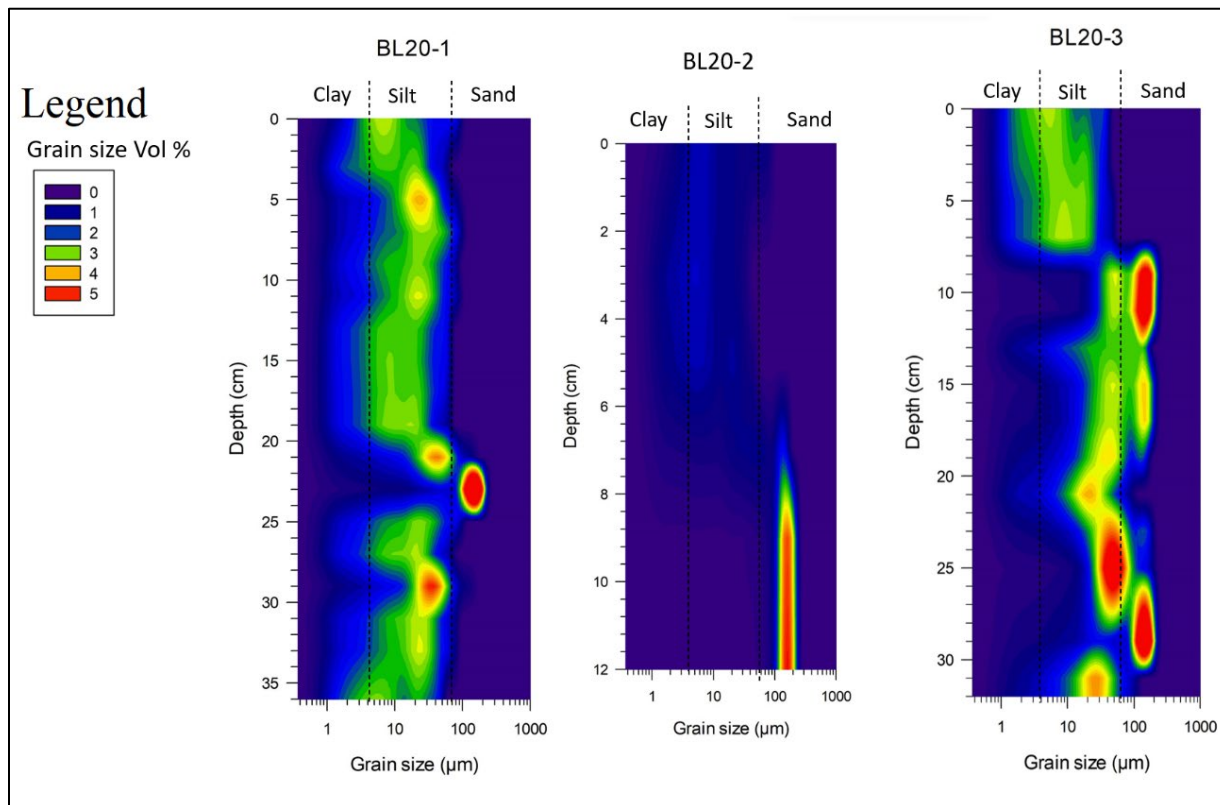


**Figure 8. Block 88 grain size color plot.**

Grain size heat maps showing the grain size volume % concentration per depth for cores within the pit.

$^7\text{Be}$ 's fast decay rate allows it only to be measured in the first few centimeters of cores from inside the pit (BL20-1, BL20-2, and BL20-3), or not at all as seen in cores taken outside the pit (BL20-4, and BL20-5) due to being predominantly very fine to fine sand. Depth of  $^7\text{Be}$  penetration ranges from 8–12 cm, averaging 10.67 cm across cores BL20-1, BL20-2, and BL20-3 (Figure 9). This shows an average of 10.67 cm is deposited within a 6-month time frame, with a deposition rate of 0.2–0.25  $\text{m yr}^{-1}$  of  $^7\text{Be}$  adhered sediment. The  $^7\text{Be}$  activity in all three cores from inside pit does not show a standard exponential decay; instead, a stepwise decay pattern is seen (Figure 9). This stepwise decay could be due to either periods of punctuated sedimentation or heavy bioturbation activity within the pit (O'Connor, 2017; Barley, 2020). Peak  $^7\text{Be}$  activity within the pit ranges from,  $3.66 \pm 0.22$  dpm/g (disintegrations per minute per gram) to  $3.58 \pm 0.22$  dpm/g, nearly identical in all peaks across the cores BL20-1, BL20-2, and BL20-3.

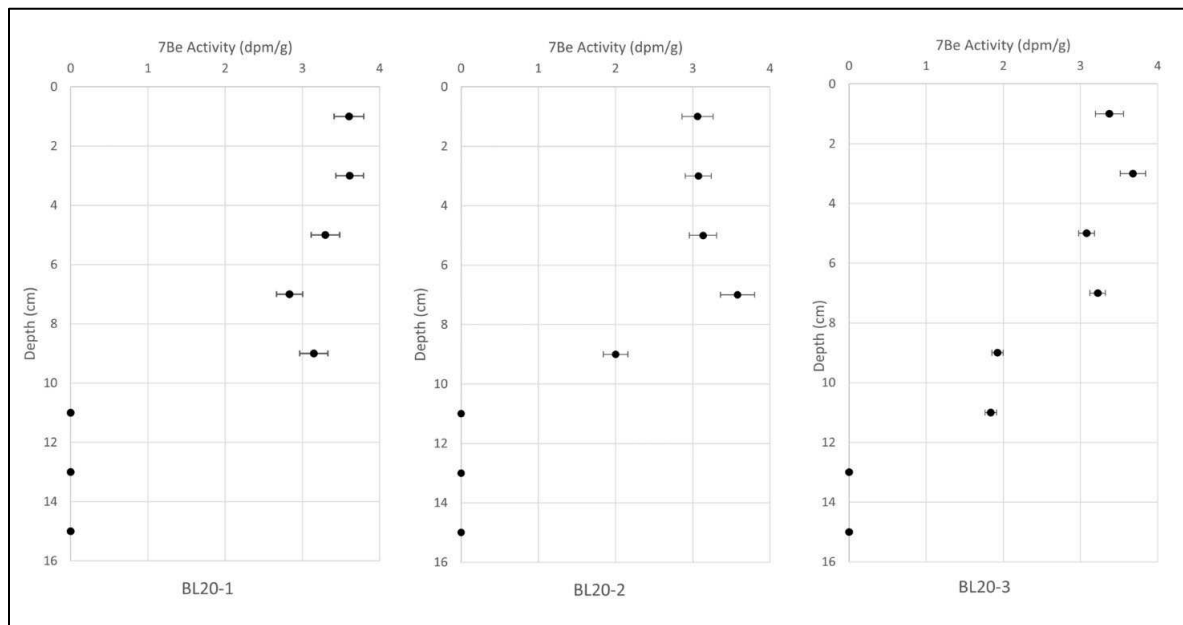


**Figure 9. Block 88's <sup>7</sup>Be activity plot.**

<sup>7</sup>Be activity (disintegrations per minute per gram) as depth (cm) increases. No <sup>7</sup>Be activity was found in cores BL20-4 nor BL20-5 due to Be-7 only attaching to fine grained particles and BL20-4 and 5 were coarser grained (sand). Published in Moran et al. (2022).

Core BL20-1 contains distinct beds (>1cm) of medium silt and finer to clay, with minor laminations (<1 cm) of coarser grained material, coarse silt and coarser up to fine sand (Figure 10). Massive bedding of silty material is observed from 24-28 cm, with many laminations present from 6-12 cm where it is capped with a bed of coarse silt and fine sand, ~1.5 cm thick. The base of the core exhibits some mottling due to either bioturbation or core extraction damage. Fining upwards sequences are noted from 12-22 cm depth. The top 6 cm of core exhibits no laminations in the silt bed with a fining upward sequence from medium to fine silt. Core BL20-2 contains distinct beds of medium silt and finer, as well as beds of coarse silt to fine sand at 5–6 cm depth (Figure 10). Laminations of finer material are present in the coarse silt beds at 7-8 cm. The top 4 cm of core has no laminations in the fine to medium silt bed. BL20-3 contains mostly beds (2-6 cm thick) of coarse silt up to fine sand, with few laminations of coarse material present in medium silt beds (Figure 10). The coarse beds contain shell fragments not seen in other cores. Some mottling is present from the base of the core up to 25 cm depth, due to either bioturbation or the core extraction process. Core BL20-3 exhibits the largest silt cover of all the cores taken within the pit, 7 cm thick composed of medium silt and finer to clay, with thin laminations of coarse silt.

The cores taken outside of the pit exhibit different sediment character than the cores taken from within the pit. Core BL20-4 shows an almost entirely fine sand make-up, with a thin lamination of silty material on the top ~1 cm of core (Figure 10). Core BL20-5 has a similar make up of almost entirely very fine to medium sand but lacking in any top silt material as compared to all the other 4 cores. Core BL20-5 exhibits a burrow created by an organism, again different from what is seen in any of the other cores.

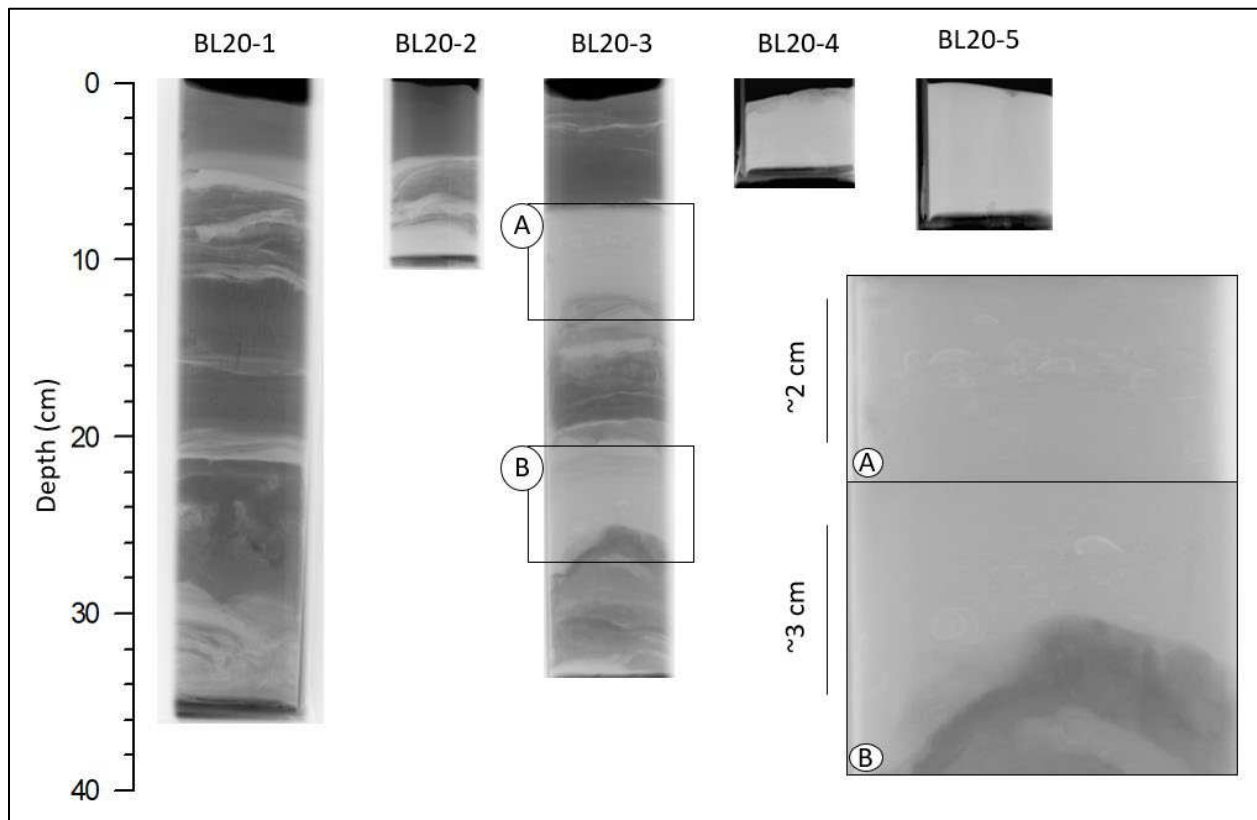


**Figure 10. Block 88 X-ray images**

X-ray Images of Cores, Lighter areas represent larger grain size (coarse silt and larger), and darker represents finer grainsize (medium silt and finer), A and B highlight the shell fragments that were able to be captured in X-ray.

### 4.3 Caminada Geophysical Results

Caminada pit geophysical results were published in Liu et al. (2022). Repeat bathymetric data in the years 2016, 2017 and 2018 shows similar overall morphology of the pit walls at Caminada Dredge Pit (CDP), but also reveals shoaling occurring inside the pit over time (Figure 11). As of July 2017 (nine months after Increment II), sediment deposition mainly occurs inside the pit; little erosion or deposition was found outside the pit. The pit depth was  $\sim 13.3$  m below sea level, compared to the  $\sim 9$  m depth of the surrounding seafloor. As of August 2018, the average depth was  $\sim 12.8$  m (Figure 11). DoD maps of the three post-dredging surveys revealed that nearly no new sediment was deposited outside of the pit, but new sediments had begun to fill the troughs and wall margins inside of the pit. The pit next to the southeastern wall showed sediment deposition. Morphological evidence for localized erosion and deposition near pit walls were observed along the northern wall (Figure 11).

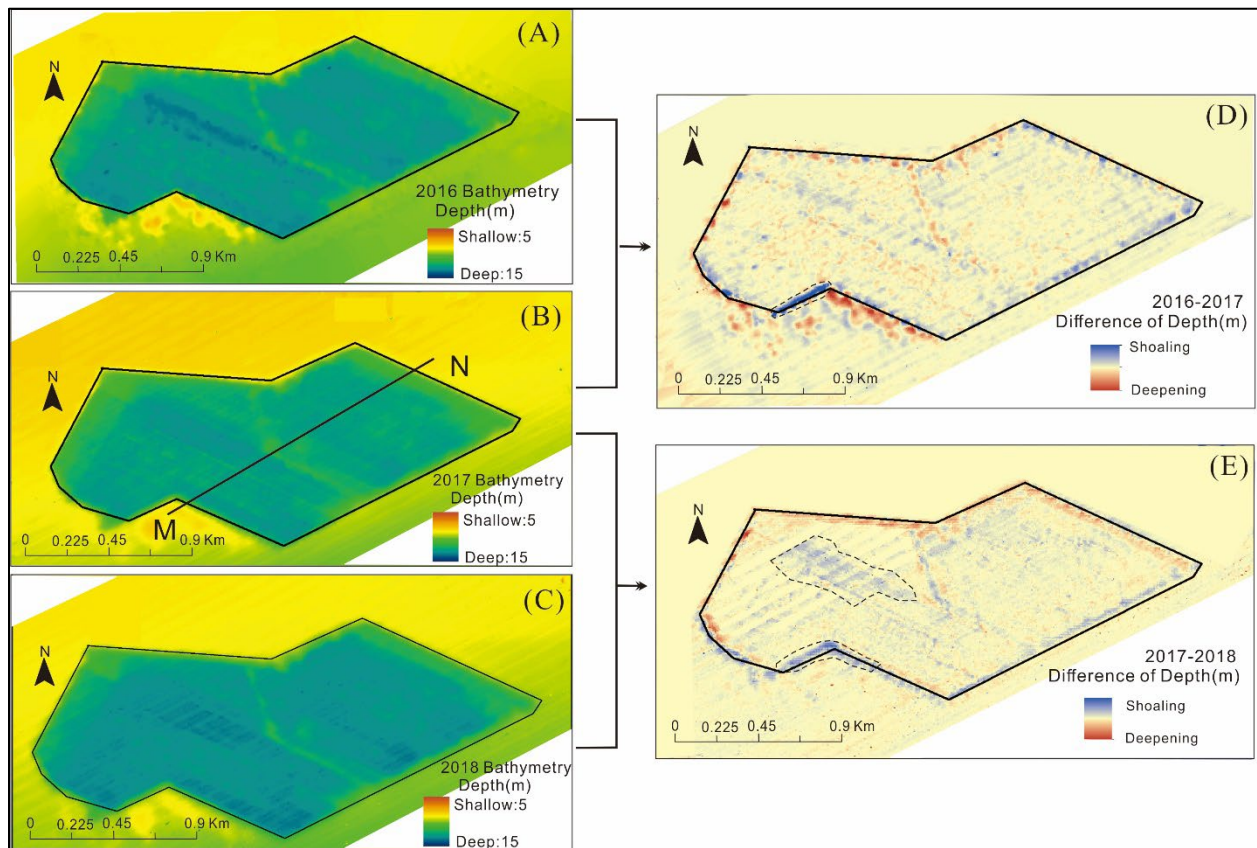


**Figure 11. Caminada bathymetry map**

(A)(B)(C) Bathymetry map of CDP in three different surveys from 10/2016, 07/2017, and 08/2018. The black polygon is the same in all images and is the margin of the bathymetry map from 2016, which is considered the reference polygon for the comparison of repeat surveys. The depth value is positive with a unit of meters. The scale of color bar is the same in panels (A)-(C). MN shows the location of the transect in Fig 4B. (D) A difference of depth between 2016 and 2017 surveys; (E) Difference of depth between 2017 and 2018 surveys. The dashed lines in D and E highlight major zones of shoaling. Values within the  $2\sigma$  range of uncertainty (0.1 m) are generally in beige and considered to have no significant depth change (from Liu et al., 2022).

An estimation of the annual sediment transportation rate is essential for predicting the evolution at CDP. The volume of infilling sediment calculated for the 9 months between the 2016 and 2017 surveys is approximately the same as the 13 months between the 2017 and 2018 surveys. This reveals that the sediment infilling rate in 2016-2017 was higher than that of 2017-2018. Post-dredging volumetric analysis of 2017-2018 indicates that CDP is presently infilling at an average rate of approximately 27,480  $\text{m}^3/\text{year}$  ( $\sim 0.15$  m/year in terms of averaged thickness of deposited sediment).

A side-scan mosaic map generated using data collected during the 2017 survey showed three lineations that were associated with lower backscatter values (Figure 12) and deeper depth. Two of the lineations were oriented northwest-southeast and were located at the center of the pit while the third was elliptical and located in the northeastern corner (Figure 12). All of these were low-bathymetric zones (defined as “troughs”) inside CDP, which are interpreted as a product of dredging activities. As of August 2018, the low-reflection troughs inside CDP increased in size continuing in the same manner as the previous depositional pattern and direction (Figure 12).

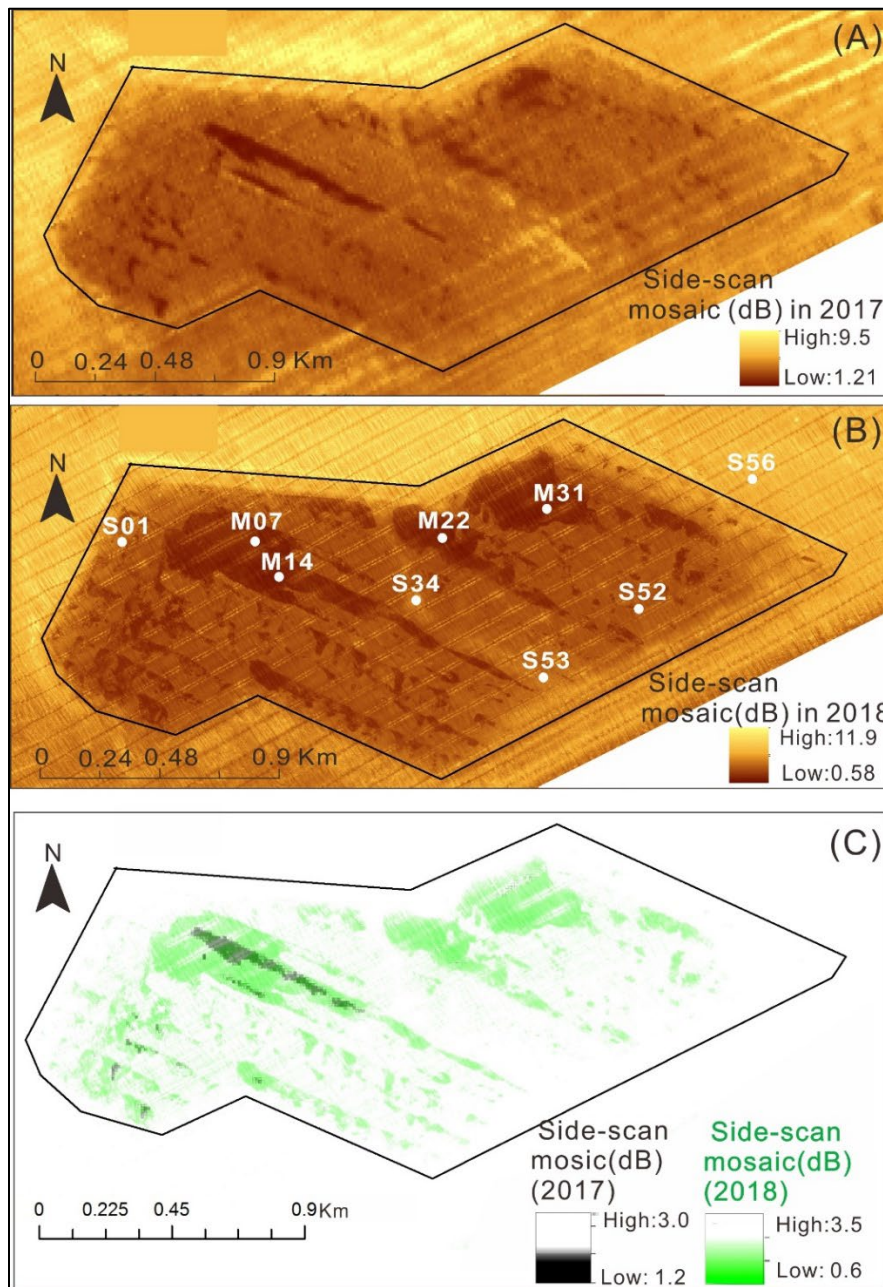


**Figure 12. Caminada sidescan map.**

(A)(B) Side-scan maps of CDP for two post-dredging surveys in 2017 and 2018. The side-scan mosaic shows the difference in backscatter values in the unit of Db (Decibel). Note the dark brown indicates the patchy mud with low backscatter values, while the bright yellow is associated with sandy sediment with high backscatter values. Note the scale of the color bars is different. The black polygon is the margin of dredge pit in 2016. White dots show the location of surficial grab sediment samples collected in 2018 with an ID number for the grain size analysis. (C) Overlaid side-scan mosaic map between years 2017 and 2018 (highlighting low backscatter values in black and green, respectively) show that muddy sediment deposited in the bathymetric lows within one year (from Liu et al., 2022).

Between the 2017 and 2018 surveys, the seafloor of CDP became flatter with the sediment infilling topographically low areas first (Figure 13). Nearly all the pit walls became less steep over the first two years after dredging. Morphological evidence for localized failure was observed near the pit walls, especially in the northern wall (Figure 13). Total wall volume loss between the 2017 and 2018 surveys

was approximately 3% (~780-824 m<sup>3</sup>/year) of the total infill volume (~27,480 m<sup>3</sup>/year) during the 13 months, 2017–2018 season. During both 2017 and 2018 surveys, it was recorded that the western walls were steeper than the eastern walls. Between the 2017 and 2018 surveys, the pit wall slope decreased from a range of ~3.3°–6.6° to a range of ~1.7°–3.6° (i.e., became gentler), which indicates a ‘relatively’ stable condition for the dredge pit between these years. Previous bathymetric survey (Penland et al., 1986) found Ship Shoal migrated landward at a rate of 7 m/year (in the east) to 15 m/year (in the west). The gradient change between the two surveys indicated CDP did not experience much outward wall migration during the 2.5 years after dredging. However, outward wall migration was found to be over 200 m in another site at Sandy Point dredge pit which is mud capped pit west of the Mississippi Delta.

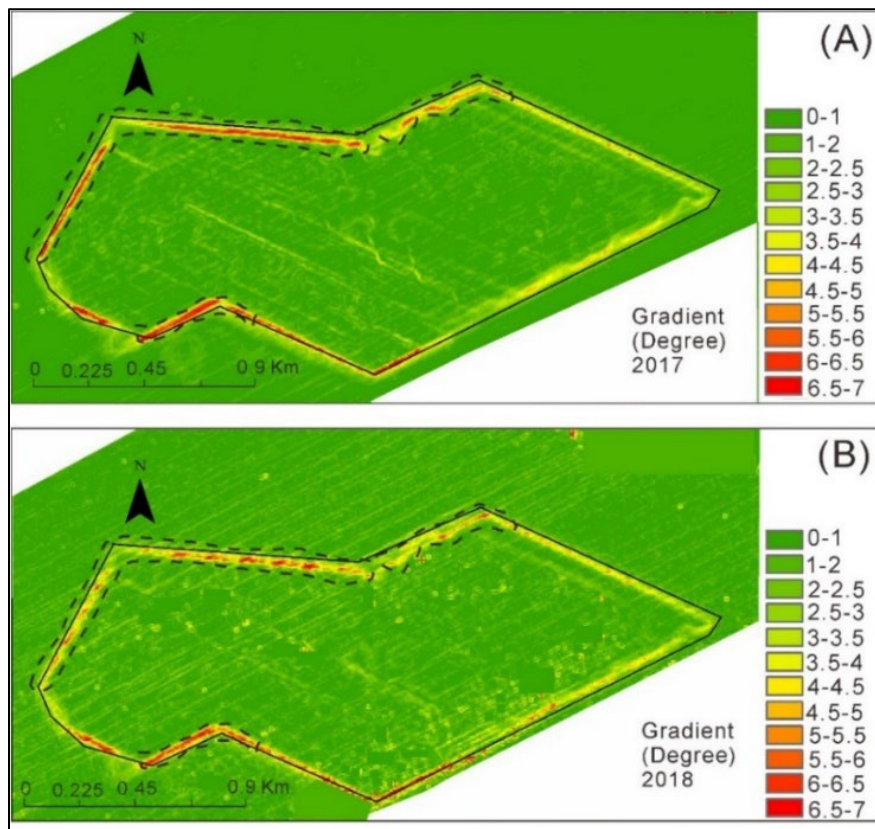


**Figure 13. Caminada slope map.**

(A)(B) Gradient maps of CDP derived from 2017 and 2018 bathymetry. Green colors represent flatter surfaces, while red colors indicate steeper surfaces. Dashed polygons are the extents of northern and southern walls used for gradient analysis, which showed decreased slopes from 2017 (red) to 2018 (yellow) (from Liu et al., 2022).

Grain size analysis of samples collected both inside and outside of the pit indicate that the sediment types have a relationship with the side-scan backscatter values. The sediment samples collected from the three low-reflection troughs (the brown zones in Figure 14) were shown to be patchy muds (Figure 14). However, the sediment samples collected from the high-reflection zones were sandy or mixed, which revealed the high backscatter values (yellow in Figure 14B).

The bathymetry of the seafloor inside of the CDP seems to have direct control over the patchy mud distribution. Figure 8A shows the troughs (blue-green color) inside of CDP during the 2017 bathymetric survey, which was a direct result of the dredging activities. At CDP, suspended muds are prone to deposition within these troughs: the boundary of patchy mud distribution in the side-scan map from the 2018 survey matches the troughs in the bathymetric data from 2017 (Figure 14).

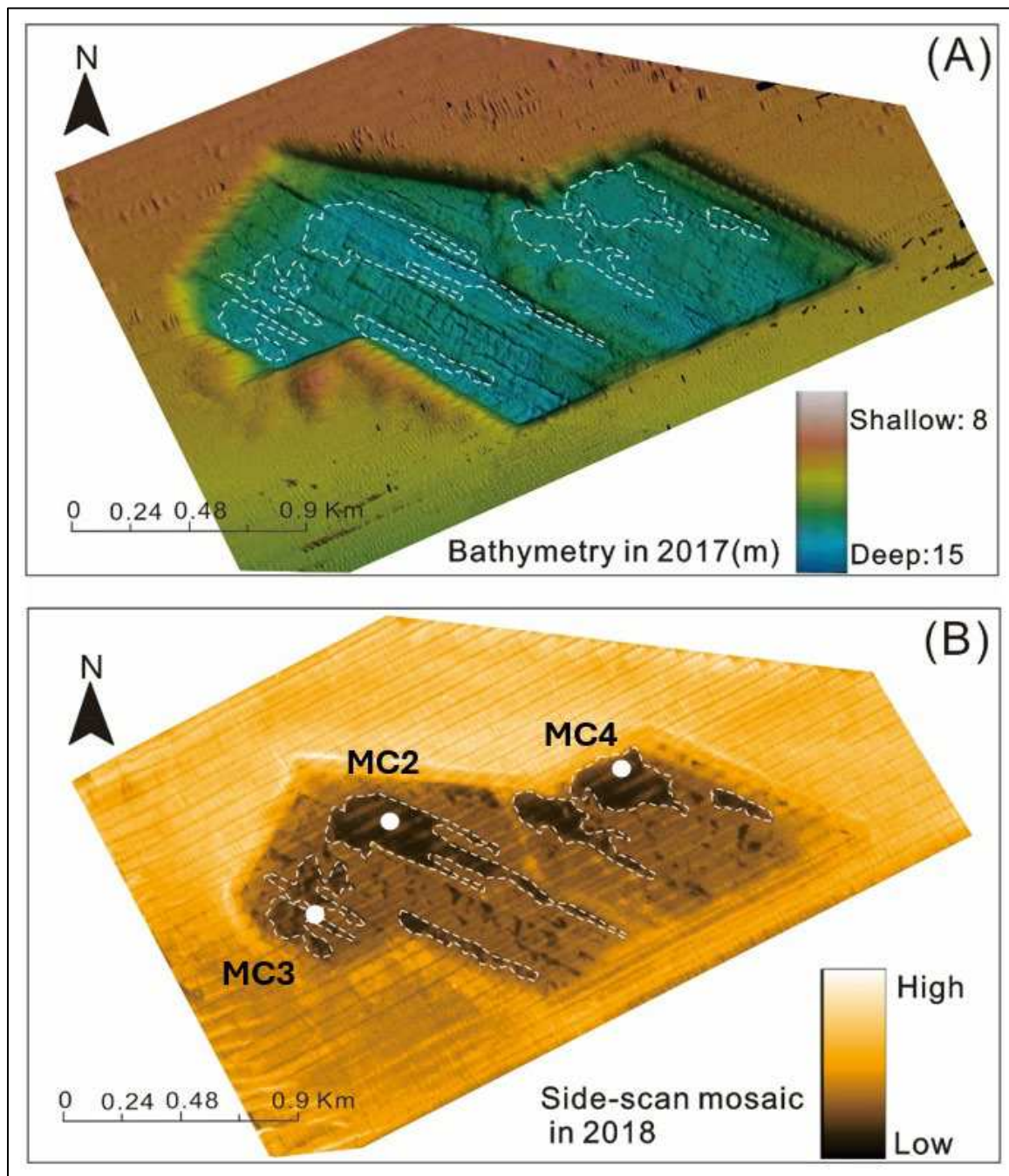


**Figure 14. Caminada bathymetry and sediment comparison.**

(A) 3-D geomorphology map of CDP from the 2017 survey with the overlaid boundaries of distribution of patchy mud in 2018. The vertical exaggeration is 32 times. White dashed polygons are extracted from (B), which are boundaries of areas with low backscatter values. It indicates the new muddy sediments are prone to deposit in the troughs inside CDP. The dark blue inside the pit indicates the topographic-low zones, which refers to the patched zones. Warm red color indicates the shoaling areas. (B) Side-scan backscatter maps of CDP for the post-dredging survey in 2018 (from Liu et al., 2022).

#### 4.4 Caminada Core Results

Caminada pit core results were published in Xue et al. (2022). Coring locations are shown in Figure 14B. Grain size analysis of shallower multicore (MC) samples (length 0.5 m) collected in 2017 indicates that the shallowest material in-filling CDP is dominated by silts at 50-80% by volume (Figure 15). On average, multicore grain sizes have a mode around medium to coarse silt, ranging from at  $4.3-6 \phi$  (16-48  $\mu\text{m}$ ; Figure 15). Only occasionally are very fine to fine sand laminations measured (averaging  $2.3-3.3 \phi$ , 100-200  $\mu\text{m}$ ; Figure 15).

Similarly, x-radiographs show packages of clays and fine silts separated by planar laminations of coarser silt to very fine sand 10–15 cm apart (see Figure 16). Specifically, in both 2017 and 2018, MC-2 and MC-4 showed 5–10 cm thick beds of fine-grained sediments (dark in X-ray image) separated by thin 1–2 cm layers of coarser grained sediments (light in X-ray image). Disruption of bedding due to soft sediment deformation can be seen, as well as bioturbation from burrows (Figure 16).

Cores collected in October 2017 showed  $^7\text{Be}$  was present at depth for three of the five cores collected from the muddy sediment in CDP. The maximum depth of  $^7\text{Be}$  penetration in 2017 ranges from 4 to 12 cm, averaging 8 cm (Figure. 17). Peak  $^7\text{Be}$  activity is observed at top-most samples and ranges from  $3.92 \pm 0.54 \text{ dpm g}^{-1}$  to  $9.14 \pm 0.70 \text{ dpm g}^{-1}$ . In 2017,  $^7\text{Be}$  activity trend shows a correlating exponential decrease with depth in these three cores. Calculated  $^7\text{Be}$  inventory ranged 0.62 to  $3.67 \text{ dpm cm}^{-2}$  and sedimentation rates from  $0.02$  to  $0.07 \text{ cm day}^{-1}$ , averaging  $\sim 0.05 \text{ cm day}^{-1}$ . Two multicores did not show beryllium in their samples: CA17-MC5 and CA17-MC11. Both cores were taken where surface sediment was sand-rich, confirmed by side scan sonar data and grain size analysis, from within a sandy area inside CDP and outside, respectively.

In the repeat coring campaign executed in May 2018, sites were reoccupied to obtain comparable seasonal sedimentation rates. Cores were similarly found to have muddy and sandy surface sediment composition.  $^7\text{Be}$  was present to depths for the same three muddy locations within CDP. Maximum depth of  $^7\text{Be}$  penetration was much deeper than in October 2017, ranging from 8 to 16 cm, averaging 12.6 cm (Figure 17). Peak  $^7\text{Be}$  activity ranges from  $5.76 \pm 0.78$  to  $9.18 \pm 1.01 \text{ dpm g}^{-1}$ . CA18- MC2 shows  $^7\text{Be}$  trend of exponential decrease with depth, with an inventory of 2.60 to  $2.85 \text{ dpm cm}^{-2}$  and sedimentation rate of  $0.15 \text{ cm day}^{-1}$  (Figure 17). CA18-MC4 displays intermittent peaks and irregular downward trend in  $^7\text{Be}$ , preventing the determination of accurate sedimentation rates in the core (Figure 17). Instead, minimum sedimentation rate is calculated by dividing depth of penetration with 4 half-lives, yielding  $0.08 \text{ cm day}^{-1}$ . The cores collected in the sandy environments inside and outside the pit (CA18-MC5 and CA18-MC11, respectively) again did not contain any detectable  $^7\text{Be}$ .

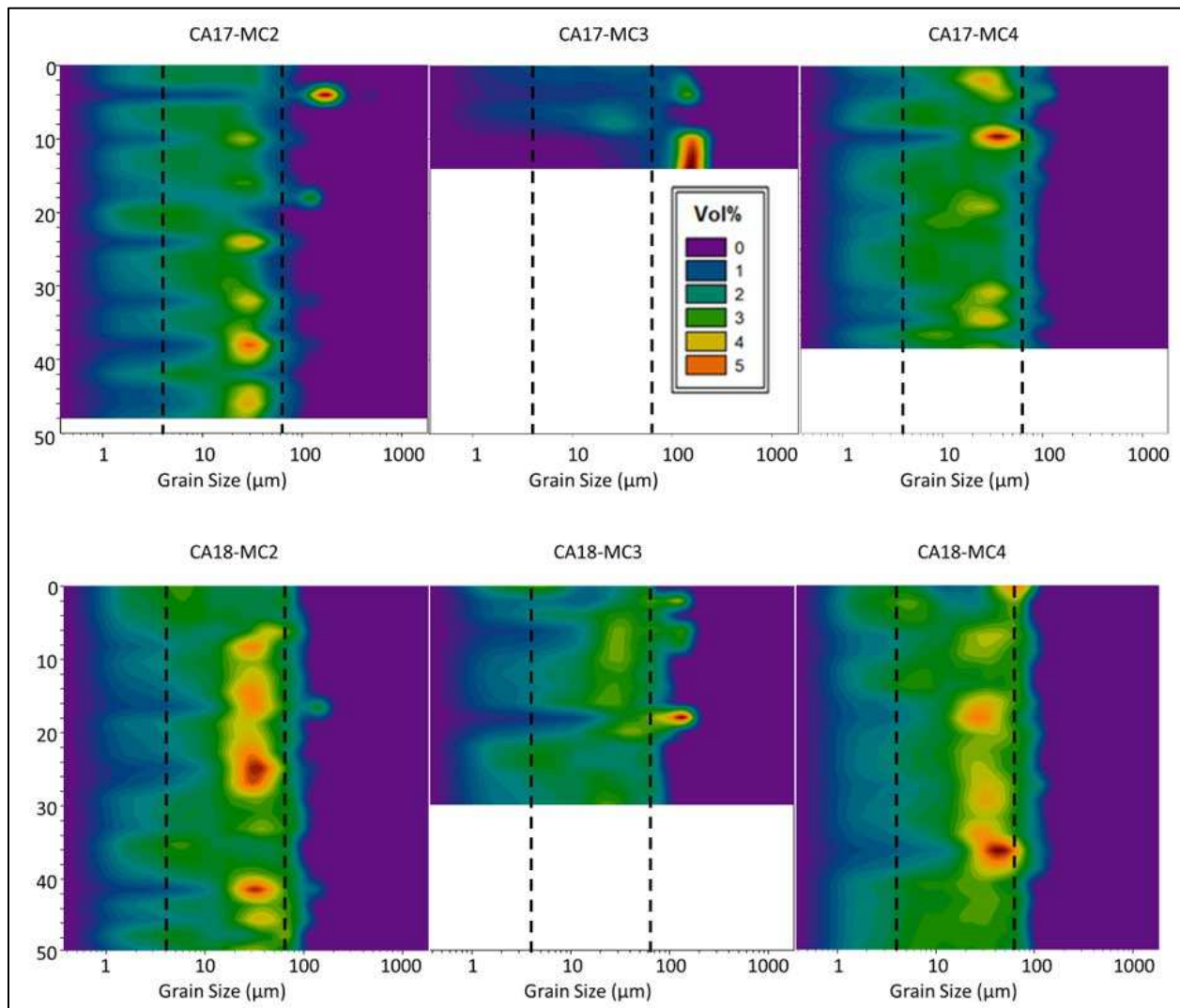


**Figure 15. Caminada grain size color plot.**

Filled-contour plots of grain size for multicore samples inside CDP in 2017 (top) and 2018 (bottom) with warmer colors corresponding to higher frequencies. Vertical dashed lines indicate divisions between clay, silt, and sand. Grain sizes are predominantly medium-coarse silt with a few laminations of very fine to fine sand (from Xue et al., 2022).

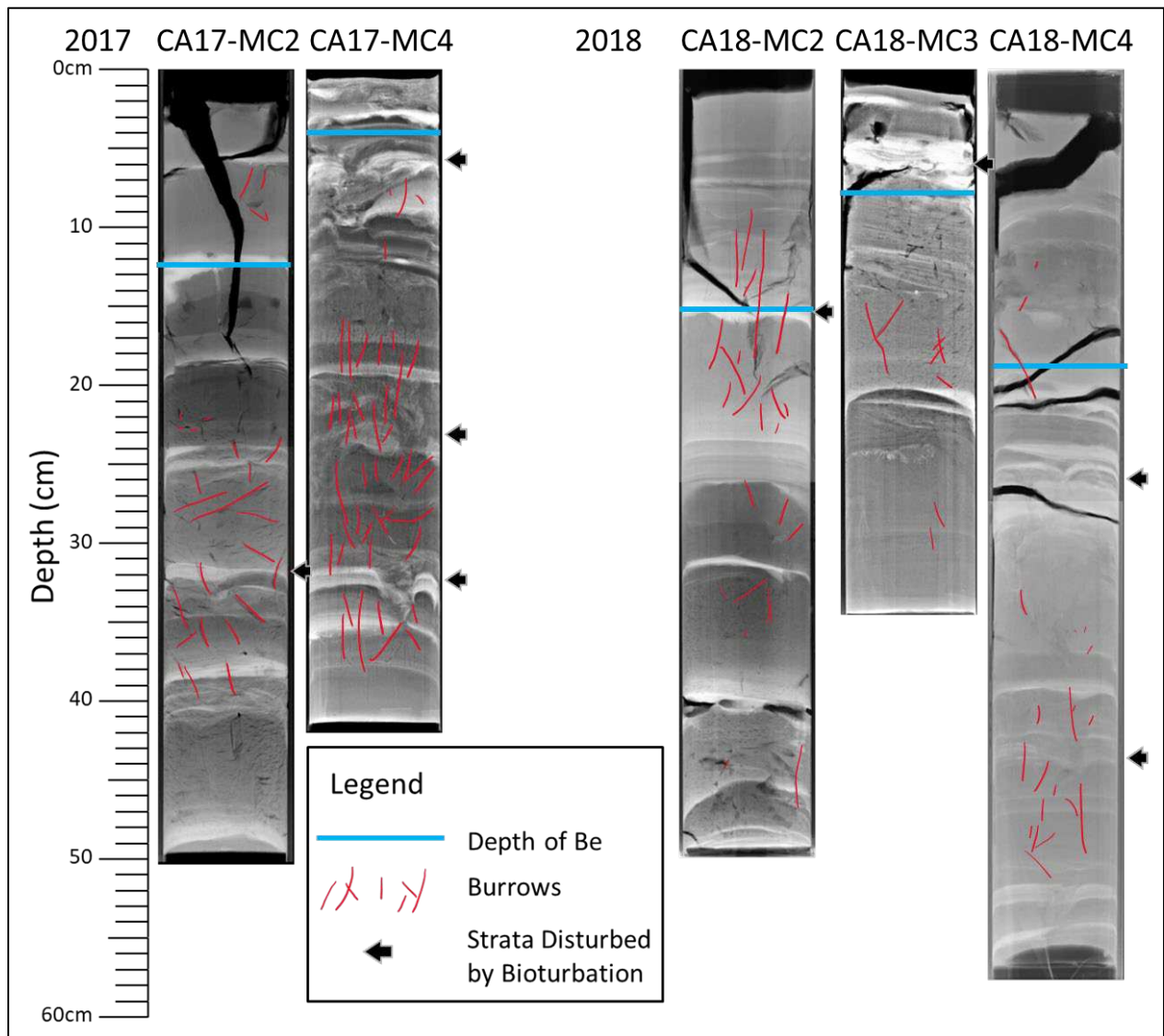


**Figure 16. Caminada x-ray images.**

Annotated x-ray images of multicores taken in 2017 and 2018. Light colors represent higher density and larger grain sizes (coarse silt/v. fine sand), while darker colors represent lower density and finer grain sizes (fine silts/clays). Blue lines for each core represent depth of  $^7\text{Be}$  penetration. Red lines are annotated burrows. Black arrows are sediments disturbed by bioturbation commonly found in the region (Bouma, 1968). Black cracks are formed by dewatering prior to x-ray analysis. See Supplemental Figure S3 for original, unannotated images (from Xue et al., 2021).

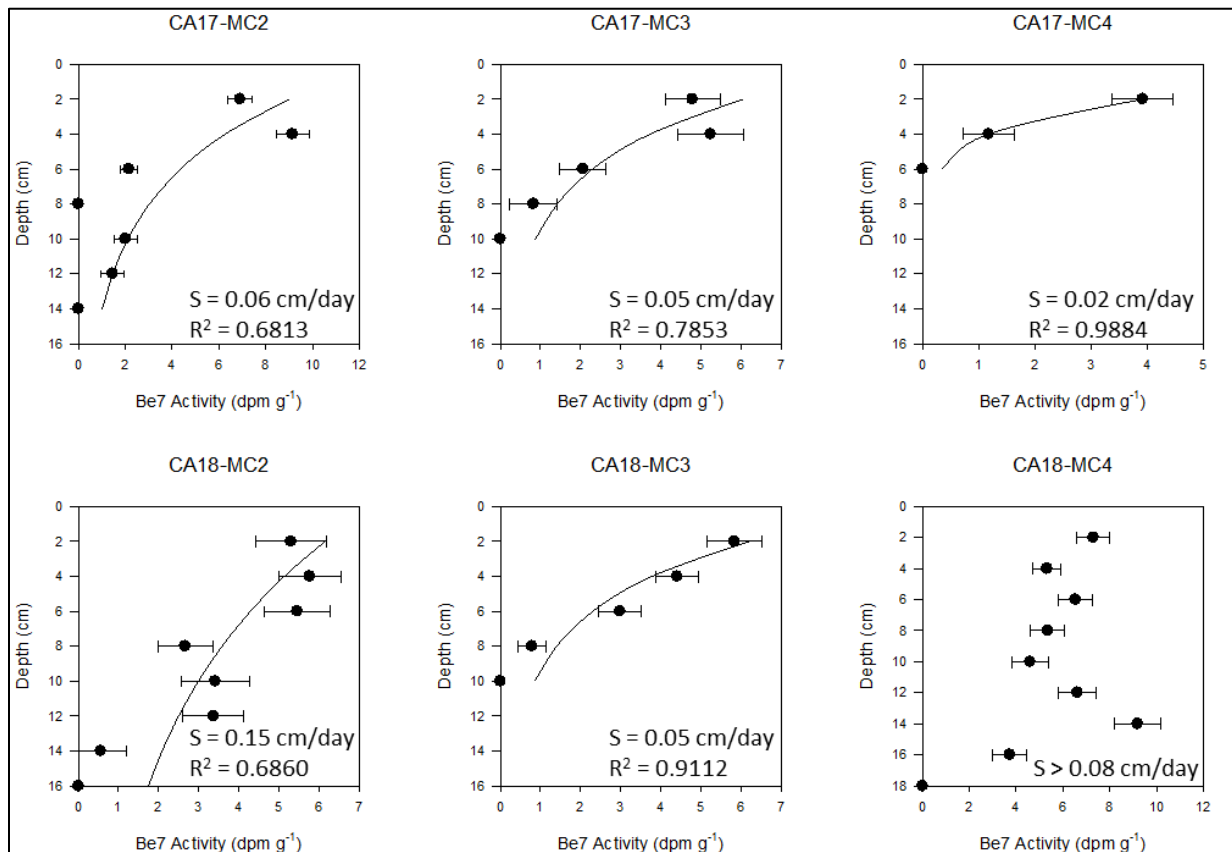
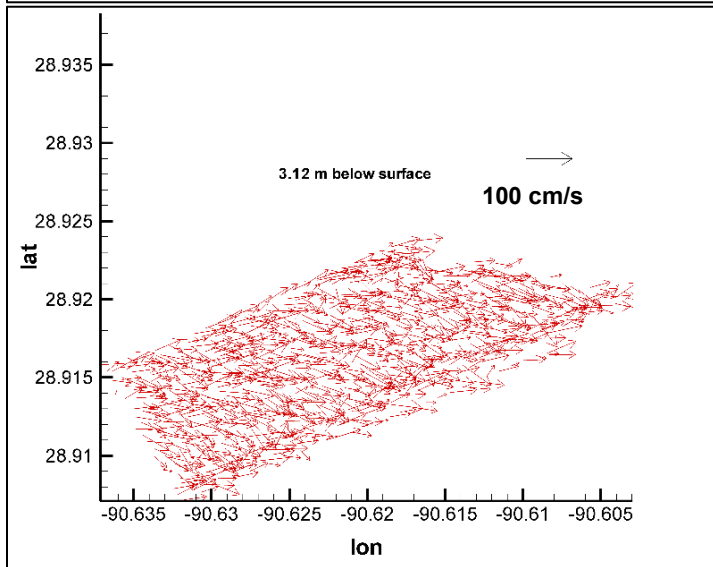
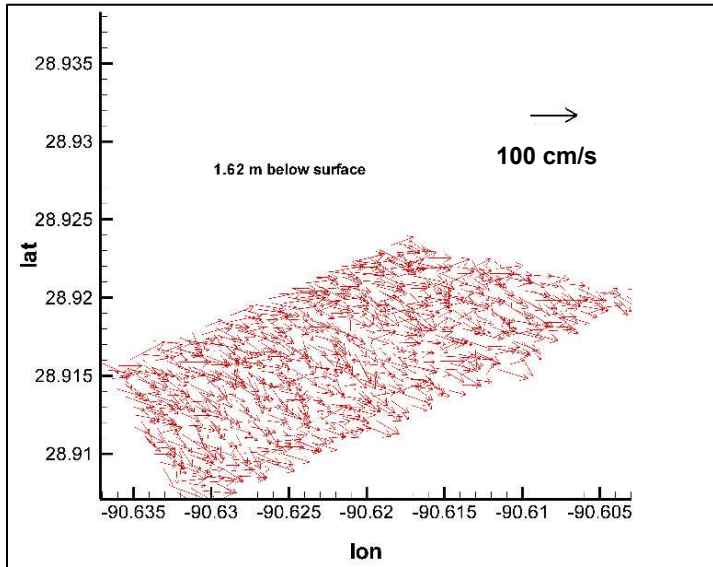


**Figure 17. Caminada Beryllium-7 activity.**

Beryllium-7 activity at depth and calculated sediment deposition rates from fall 2017 (top) and spring 2018 (bottom) at locations 2, 3 and 4. Note CA18-MC4 has slightly greater depth of penetration (from Xue et al., 2022).

## 4.5 Caminada ADCP Results

The topography of the seafloor inside Caminada Dredge Pit seems to have a direct relationship with the mud distribution. Figure 14 shows the depression zones inside the pit 2017 survey, which was the footprint of cutting/dredging sequence. Suspended mud was prone to deposit in the topography-low areas shown in Figure 14. Figure 18 shows the 3-D velocity structure of ADCP velocities over the Caminada pit at three depths during July 25, 2017. The dominant currents at 1.62 m and 3.12 m below sea surface both moved eastward whereas the bottom current directions are random.



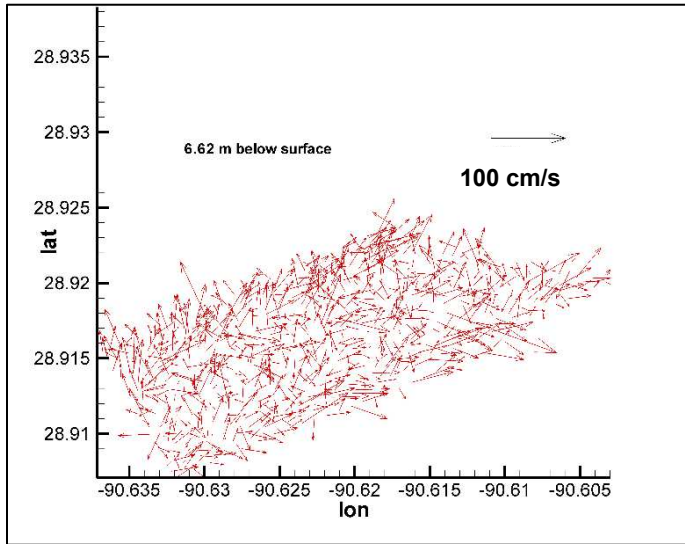


**Figure 18. Caminada ADCP velocity.**

Velocity vectors of ADCP data collected at Caminada pit during July 25, 2017. The three panels are 1.62, 3.12, and 6.62m below sea surface in top, middle and bottom panels, respectively.

## 5 Discussion and Conclusions

### 5.1 Sediment Transport Processes

The infilling of the CDP is not primarily composed of ambient Ship Shoal sand, as previously hypothesized (Nairn et al., 2005). Instead, analysis reveals a significant absence of sand within the infilled material in the interior of the dredge pit. Findings from this study indicate that the infill comprises mainly of fine to medium silts, occasionally interspersed with laminations of coarser silt and sparse very fine sand laminations. Through the presence of sediments containing  $^7\text{Be}$  and grain size analysis of cores extracted from within the CDP, it was determined that the infill is sourced from a combination of the Atchafalaya and Mississippi River plumes. In addition, it is suggested that storm events may resuspend fine-grained material from the shelf and local bays, transporting it to the dredge pit. Furthermore, CDP is infilling at a slower rate (~5 times less) than numerical modeling predicted (Nairn et al. 2005; Liu et al. 2020b) or exhibited by paleo-channel dredge pits more proximal to the Atchafalaya and Mississippi River mouths (Sandy Point and Raccoon Island ~90% more: average sedimentation rates  $0.145\text{--}0.24\text{ cm day}^{-1}$ , O'Connor, 2017; vs. Caminada  $0.05\text{--}0.10\text{ cm day}^{-1}$ ). Nairn et al. (2005) proposed that sandy dredge pits would experience accelerated sedimentation rates compared to paleo-channels with mud overburden, attributed to bedload transport of sand outside the pit and subsequent deposition inside. However, our recent observations from 2017 to 2018 indicate an increase in areas covered by fine sediments overlaying the original Ship Shoal sands (Liu et al., 2019).

In 2017, 4–12 cm of sediments were deposited within a 5–6-month period in low lying areas in CDP. Sedimentation rates are calculated to be  $0.02\text{--}0.06\text{ cm day}^{-1}$ . During repeat coring in 2018, 8–16 cm of sediments were deposited and sedimentation rates calculated to be  $0.05\text{--}0.15\text{ cm day}^{-1}$ . Vibracore samples collected in 2017 and 2018 confirmed new silts and clays with grain sizes  $4.3\text{--}6\phi$  ( $16\text{--}48\mu\text{m}$ ) deposited overlying coarser original Ship Shoal sand with grain sizes  $2.3\text{--}3.3\phi$  ( $100\text{--}200\mu\text{m}$ ) and older pro-delta deposits. The average  $^7\text{Be}$  inventory remained relatively consistent, although there were greater spatial variations observed in 2017. The deposition of clays and fine silts in the dredge pit appears to be intermittent and is likely sourced from the Atchafalaya and Mississippi River plumes, as well as from resuspension from the shelf and bays. This is supported by satellite imagery showing the plume geometry as well. Sediments from the Atchafalaya plume extend southeastward to reach the CDP, particularly following winter or tropical storms. The resuspension and redeposition of sediments during these higher energy events likely resulted in the formation of coarse silt laminations. It appears that wall slope failure is a minor contributor to sediment in the interior portions of the dredge pit, as evidenced by the absence of original Ship Shoal sand material in core deposits.

DoD maps from three post-dredging surveys show minimal new net sediment deposition outside of the pit, while new sediment was deposited inside the pit. Volumetric analysis conducted after dredging indicates that the pit is currently filling at an average rate of  $0.15 (\pm 0.05)\text{ m/yr}$ . The topography of the seafloor inside the pit is directly related to the distribution of patchy mud. Side-scan mosaic maps revealed that troughs inside the pit were infilled with mud within two years post-dredging. As a result, the seafloor inside the CDP became smoother and flatter due to sediment infilling. In the two years following dredging, the walls of the pit became gentler, and sediment erosion and deposition were observed near the walls. The outer migrations of the CDP's walls were less than a few meters, suggesting that the current setback buffer distances of ~300 m from planned pipelines could potentially be reduced.

The rate of sediment infilling in the CDP, like many dredge pits across the country, is significantly influenced by sediment availability. Comparisons of the amount of sediment removed and the rate of subsequent infilling can be made with published data from other mixed dredge pits in various geographic and geological settings. For instance, Byrnes et al. (2004) conducted modeling of nearshore wave and

sediment transport under post-dredging conditions. They found that sand mining at multiple sites, including New Jersey and Mobile Outer Mound, Alabama, had minimal environmental impact on sediment dynamics and wave height. Our results indicate the pit has a sediment infilling rate that is  $\sim 27.5 \times 10^3 \text{ m}^3/\text{year}$ , while dredge pits in Mobile Outer Mound have slower sediment infilling rates ( $13.5 \times 10^3 \text{ m}^3/\text{year}$ ) due to insufficient sediment supply from the local major rivers and a low longshore sediment transport rate (Byrnes et al., 2004). The disparity in infilling rates between dredge pits in Alabama and Louisiana highlights the significance of proximity to sediment sources in the infilling process. Comparing the infilling rates of mud-capped dredge pits in Louisiana (15 years in Obelcz et al., 2018; 13 years in Robichaux et al., 2020; and 5 years in Liu et al., 2020a and Bales et al., 2021), CDP has a relatively low sediment infilling rate: assuming a constant slow infilling rate of  $0.15 (\pm 0.05) \text{ m/yr}$  and an average excavation depth of 4.3 m, it would take 28.7 years to fill up this pit. The presence of mud-capped dredge pits near major river sources underscores the importance of proximity to fluvial sediment sources in the infilling process. However, the CDP, with a sand volume of  $9.07 \times 10^6 \text{ m}^3$ , differs significantly from smaller pits like those in Palm Beach, Florida ( $0.93 \times 10^6 \text{ m}^3$ ), which are predicted to fill up within a few years (Kennedy et al., 2009). This suggests that the excavation volume of dredge pits can also be a crucial factor in determining the filling time.

Previous studies suggest that hurricanes can play a significant role in sediment infilling of dredge pits (Byrnes et al., 2004; Kennedy et al., 2009). Kennedy et al. (2009) conducted bathymetric surveys before and after hurricanes in 2005 at sandy pits such as Corson Inlet (New Jersey) and Palm Beach (Florida), finding that the pits captured sediments equivalent to up to four years of net longshore transport during hurricane seasons. However, Liu et al. (2020b) modeled sediment transport near Ship Shoal for the years 2017–2018 and found hurricanes contributed less than 10% of the infilling sediments in both the Caminada and Raccoon Island dredge pits from July 2017 to October 2018, mainly due to their far distances to the eyes of hurricanes. The CDP was dredged in sand-dominated Ship Shoal, resulting in a significantly lower infilling rate than predicted by Nairn et al. (2005). While mud is beneficial for marsh restoration, it is not considered a quality sediment resource for barrier island restoration. The fine-grained nature of the infilling sediment of the CDP results in a non-renewable resource for high-quality sand for future restoration efforts. Continued collection of time-series geophysical, hydrodynamic, and physical data is essential for better understanding the infilling process. Additionally, the quantity of sand available for restoration projects is substantially reduced due to setback buffer distances required by regulatory agencies for subsea oil and gas infrastructures, as well as cultural resource concerns regarding dredging in these shoals. The relatively small outer migrations (a few meters) of walls in the CDP suggest that current setback buffer distances of  $\sim 300 \text{ m}$  from planned pipelines could potentially be reduced. Longer-term data (e.g., 10- and 20-years post-dredging) are necessary to make recommendations on setback buffer distances.

## 5.2 Conceptual Pit Morphology Model

Based on our findings, Liu et al. (2022) presented a conceptual model to represent the sediment infilling process within sandy dredge pits. The first and second phases occur rapidly when strong currents and waves continuously impact the pit: eroded sediments from pit margin are transported into the dredge pit under the controls of short-timescale currents, tides, and waves. After initial rapid failing and stabilization of the pit walls, far-field suspended muddy sediment from rivers, and sandy sediment from local erosion dominate infilling volumetrically (Figure 19A; Liu et al., 2022). Muddy sediment can be sourced from the plumes from the Atchafalaya or Mississippi rivers, or advection of concentrated benthic suspension that is seasonally deposited in the nearshore environment (Stone et al., 2009). These muddy sediments likely blanket the pit bottom as a sheet-like layer (Figure 10B; Liu et al., 2022). As a result, sediments deposited inside the pit (both sand and mud) are re-suspended by local currents or storm winds that generate high bottom shear stress, strong bottom sediment suspension, and vertical mixing within the dredge pit (Figure

19C). The finest of these suspended sediments (mud) are then prone to deposit in the troughs inside the pit (Figure 19D). Over time, freshly deposited sediments experience compaction and consolidation. These processes are cyclic and restart every time far-field muddy sediment or local sandy sediment is transported into the dredge pit (Liu et al., 2022).

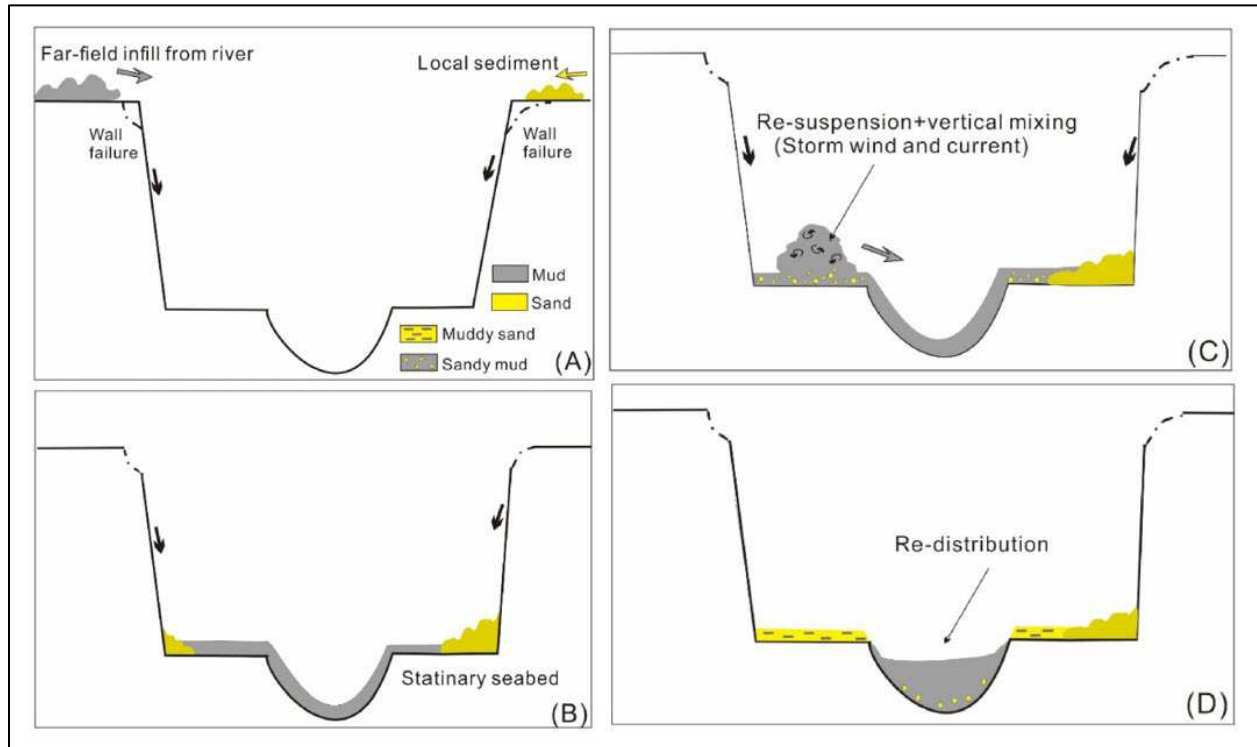


**Figure 19. Conceptual pit morphology model.**

Schematic evolution model of South Pelto Dredge Pit near a fine-grained sediment source. The graphs are dimensionless and not to scale. (A) and (B) take place when muddy sediment is transported and deposited in the pit. (C) The third phase of evolution, during which local currents, waves, and storms drive sediment re-suspension and vertical mixing. (D) The last phase shows mixed sediments re-distribution inside of the pit (from Liu et al., 2022).

### 5.3 Recommendations and Future Work

Nairn et al. (2005) used a 1-D analytical model developed by Ribberink et al. (2005) to estimate the rate of migration and infilling for a dredge pit excavated into a sandy substrate in deep water, where the dredge pit depth is of the same order of magnitude as the water depth. This model describes the evolution and infilling of sandy pits as a migrating wave, driven by the presence of the pit on a migrating sand body. The rate of shoal migration, between 2.3 and 3.5 m year<sup>-1</sup>, was determined using bathymetry data from 1936 to 2002, measuring the landward shift of the steep shoreward slope over the 66-year period to generate an average migration value for the model.

However, analysis of our three years of bathymetric data shows that Ship Shoal is not continuously migrating, contradicting one of the base assumptions of the chosen model. This assumption appears to be only applicable during years of above-average wave heights (i.e. > 1.1m; Stone et al., 2004; Nairn et al.,

2007); in the region when the wave base is extended below ~20 m causing resuspension of shoal sediments and forcing the shoal to migrate landward.

Furthermore, Nairn's model estimates were calculated prior to the excavation of the Block 88 dredge pit and were based on the proposed parameters of the pit. However, as the project progressed, the shape and dimensions of Block 88 evolved, and the final pit differed from the modeled pit in several aspects, resembling the model only in the final excavation depth. This divergence from the original model led to several challenges when attempting to assess the validity of the model. Block 88 turned out to be more than double the width of the proposed pit that Nairn et al. (2005) had modeled to determine sediment infilling rates. Across the narrowest width of Block 88, the pit is ~36% (230 m) wider than the largest width dimension modeled, and the greatest length of Block 88 is ~17% (285 m) longer than the modeled pit making a direct comparison of expected vs measured values impractical. However, the infilling rate for Block 88, regardless of size, has been overestimated.

Moreover, the sedimentation rates of 0.2-0.25 m yr<sup>-1</sup> for Block 88 and 0.18-0.37 m yr<sup>-1</sup> for Caminada (Barley, 2020; Xue et al., 2022) are significantly lower than the 0.86 m yr<sup>-1</sup> predicted by Nairn et al. (2005). There is a possibility that the gross rate of sediment transport was overestimated, leading to an inaccurate model for the infilling rate of the pit bottom. Nairn and colleagues noted that the value they calculated for Ship Shoal (150 m<sup>3</sup> m<sup>-1</sup> yr<sup>-1</sup>) is towards the high end of values. This could be due to an overestimate of sediment concentration in different scenarios or the use of an inappropriate model, given Ship Shoal's punctuated migration landward.

Our results in Block 88 pit suggest that future dredge pits can be designed to capitalize on the environmental conditions at Ship Shoal, promoting sediment capture. The choice of dredging equipment shapes the bottom morphology of the pit, which in turn influences the distribution of sediment accumulation within the pit. For example, cutterhead dredging equipment was used, creating parallel, elongated troughs perpendicular to the dominant current direction. This initial surface morphology established a ridge-trough system that effectively trapped mud. Additionally, Block 88's long axis was oriented roughly perpendicular to the east-west longshore current, leading to significant accumulation of sandy sediments along the eastern pit wall over the three-year study period. These findings suggest that long, narrow dredge pits with rough bottoms and long axes perpendicular to the longshore current would be an optimal design for sediment trapping on Ship Shoal, potentially facilitating their re-use for coastal restoration efforts.

The recent dredging projects at Block 88 and Caminada pits offer valuable insights into how the location, geometry, and type of borrow area influence the infilling sediment type and rate. The infilling at Block 88 highlights that the pit orientation relative to longshore transport is a key factor in successfully trapping larger grain sizes (sands), while the microtopography of the pit bottom dictates the trapping of finer grain sizes (muds). Future pits excavated at Ship Shoal and similar shallow submarine shoals in the Northern Gulf of Mexico should have their long axis perpendicular to the longshore sediment transport direction to maximize natural trapping of bed load. This approach could lead to increased interception, trapping, and potential reuse of bed load and sand. The past modeling work for Block 88 (Nairn et al., 2005) overestimated the sediment infilling rate, suggesting that future models should be improved to assess whether the dredge pit dimensions or the model type need reassessment. It is crucial that both suspended load and bed load are explicitly modeled, as this study demonstrates that the sediment accumulation rate and the gross sediment transport rate assumed for Ship Shoal were too high. These findings will enhance decision-making regarding seafloor stability and the protection of environmental and cultural resources, while also providing valuable datasets for better management of limited sand resources.

Our results also suggest an urgent need for new infilling models for future coastal restoration efforts, particularly in sandy dredge pit environments. Furthermore, the infilling of the dredge pit with finer-grained sediments implies that the quality sand resources for sandy shoal restoration in this location are

not renewable. Additionally, given the substantial deposition of new silt and clay within the CDP, further research is warranted to understand the biochemical impacts of a muddy depression within Ship Shoal. This research is crucial for characterizing the dredging impacts on benthic ecological communities and water quality in the area.

When comparing sandy dredge disposal pits (SDDPs) on Ship Shoal to muddy dredge disposal pits (MCDPs) along Louisiana's coast, it becomes evident that these two types of dredge pits exhibit different behaviors and infilling rates. Studies by Barley (2020), Xue et al. (2022), and Liu et al. (2022) on SDDPs, and O'Connor (2017), Obelcz et al. (2018), Barley (2020), Liu et al. (2020b), and Robichaux et al. (2020) on MCDPs, show that MCDPs have higher infilling rates of 0.5–2 m yr<sup>-1</sup> compared to the lower rates of 0.1–0.3 m yr<sup>-1</sup> for SDDPs in Louisiana. This difference can be attributed to the locations of the dredge pits, sediment availability, and bathymetry. MCDPs are often situated in bathymetric lows near modern, active river systems, making them effective sediment traps. In contrast, SDDPs on Ship Shoal are located on sediment-starved bathymetric highs, where it requires more energy to transport suspended sediments than in the surrounding areas, thus limiting sediment accumulation. Additionally, SDDPs tend to experience more pit wall failure than MCDPs, leading to a gentler slope over time, as observed 2-3 years following dredging. This is logical due to the cohesive nature of muds and the higher angle of repose for cohesive sediments.

For future dredge pit projects on Ship Shoal, it would be beneficial to reevaluate the model developed for Block 88 by Nairn et al. (2005) with updated inputs, including newly observed sedimentation rates, actual dredge pit dimensions, shoal migration rates, and possibly a smaller gross rate of sediment transport. It would also be advantageous to explore the practicality of combining the 1-D analytical models developed for SDDPs and MCDPs, as it appears that both bedload and suspended load play roles on Ship Shoal.

## References

- Barley M. 2020. Seasonal infilling and sedimentary characteristics in sandy versus muddy coastal borrow areas on the Louisiana continental shelf, USA [thesis]. Baton Rouge: Louisiana State University.
- Bouma AH. 1968. Distribution of minor structures in Gulf of Mexico sediments. *Gulf Coast Assoc Geol Soc Trans.* 18:26–33.
- Breland C, Miller B, & Dartez S. 2015. Barrier Island Restoration Using GOM Shoal Sands: Success Stories, Lessons Learned. Poster presented at: Gulf of Mexico Offshore Sand Management Working Group Meeting; 13 October 2015; New Orleans, LA.
- Byrnes MR, Richard MH, Tim DT, & David BS. 2004. Physical and biological effects of sand mining offshore Alabama, USA. *J Coast Res.* 20(1):6–24.
- Kennedy AB, Slatton KC, Starek M, et al. 2009. Hurricane response of nearshore borrow pits from airborne bathymetric lidar. *J Water Port Coast Ocean Eng.* 136(1):46–58.
- Kulp M, Penland S, Ramsey K. 2001. Ship Shoal: sand resource synthesis report. United States, New Orleans (LA): Coastal Research Laboratory, Department of Geology and Geophysics, University of New Orleans (US).
- Liu H, Xu K, Wilson C, et al. 2022. Geomorphologic change and patchy mud infilling in a sandy dredge pit in eastern Ship Shoal, Louisiana shelf, USA. *Geomorphology.* 396:107983.
- Liu H, Xu K, Ou Y, et al. 2020. Sediment transport near Ship Shoal for coastal restoration in the Louisiana shelf: A model estimate of the year 2017–2018. *Water.* 12(8):2212.
- Liu H, Xu K, Wilson C. 2020. Sediment infilling and geomorphological change of a mud-capped Raccoon Island dredge pit near Ship Shoal of Louisiana shelf. *Estuar Coast Shelf Sci.* 245:106979.
- Liu H, Xu K, Li B, et al. 2019. Sediment identification using machine learning classifiers in a mixed-texture dredge pit of Louisiana shelf for coastal restoration. *Water.* 11:1257.
- Moran K, Xu KH, Wilson C, Lopez G. 2022. Contrasting modes of sediment infilling and geomorphic change within a sand dominated dredge pit on the inner Louisiana shelf. *Estuar Coast Shelf Sci.* 278:108127.
- Munnely R. 2016. Fishes Associated with Oil and Gas Platforms In Louisiana’s River-Influenced Nearshore Waters [thesis]. Baton Rouge: Louisiana State University.
- Nairn RB, Lu Q, Langendyk SK, & Michel J. 2005. A study to Address the Issue of Seafloor Stability and the Impact on Oil and Gas Infrastructure in the Gulf of Mexico. New Orleans (LA): U.S. Department of Interior, Minerals Management Service, Gulf of Mexico OCS Region. 179 p. Study No.: OCS Study MMS 2005-043.
- Nairn RB, Lu Q, Langendyk SK, Hayes MO, Montagna PA, Palmer TA, & Powers SP. 2007. Examination of the Physical and Biological Implications of Using Buried Channel Deposits and other Non-Topographic Offshore Features as Beach Nourishment Material. New Orleans (LA): U.S. Department of Interior, Minerals Management Service, Gulf of Mexico OCS Region. 231 p. Study No.: OCS Study MMS 2007-048.
- Nittrouer JA, Allison MA, & Campanella R. 2008. Bedform transport rates for the lowermost Mississippi River. *J Geophys Res Earth Surf.* 113(F3).

- Obelcz J, Xu K, Bentley S, O'Connor M, & Miner M. 2018. Mud-capped dredge pits: an experiment of opportunity for characterizing cohesive sediment transport and slope stability in the northern Gulf of Mexico. *Estuar Coast Shelf Sci.* 208:161–169.
- O'Connor M. 2017. Sediment Infilling of Louisiana Continental-shelf Dredge Pits: A Record of Sedimentary Processes in The Northern Gulf of Mexico [thesis]. Baton Rouge: Louisiana State University.
- Penland S, McBride RA, Williams SJ, Kindinger JL, & Boyd R. 1989. Holocene sand shoals offshore of the Mississippi River delta plain. *Gulf Coast Assoc Geol Soc Trans.* 39:471-480.
- Penland S, Suter JR, & Moslow TF. 1986. Inner-shelf shoal sedimentary facies and sequences: Ship Shoal, northern Gulf of Mexico, Louisiana Geological Survey, Baton Rouge, 114p.
- Research Planning, Inc., Tidewater Atlantic Research, Inc., & Baird & Associates Ltd. 2004. Archaeological Damage from Offshore Dredging: Recommendations for Pre-Operational Surveys and Mitigation During Dredging to Avoid Adverse Impacts. Herndon (VA): U.S. Department of the Interior, Minerals Management Service, Sand and Gravel Unit, Leasing Division. 75 p. Study No.: OCS Report MMS 2004-005.
- Ribberink JS, Roos PC, Hulscher SJ. 2005. Morphodynamics of Trenches and Pits under the Influence of Currents and Waves-Simple Engineering Formulas. In: *Coastal Dynamics 2005: State of the Practice.* 2005:1-13.
- Robichaux P, Xu K, Bentley SJ, Miner MD, & Xue ZG. 2020. Morphological evolution of a mud-capped dredge pit on the Louisiana shelf: Nonlinear infilling and continuing consolidation. *Geomorphology.* 354:107030.
- Stone GW, Condrey RE, Fleeger JW, & Khalil SM. 2009. Environmental investigation of the long-term use of Ship Shoal sand resources for large-scale beach and coastal restoration in Louisiana. New Orleans (LA): U.S. Department of Interior, Minerals Management Service, Gulf of Mexico OCS Region. 278 p. Study No.: OCS Study, MMS 2009-024.
- Stone GW, Pepper DA, Xu J, & Zhang X. 2004. Ship Shoal as a prospective borrow site for barrier island restoration, coastal south-central Louisiana, USA: numerical wave modeling and field measurements of hydrodynamics and sediment transport. *J Coast Res.* 20(1):70–88.
- Xu KH, Obelcz J, Bentley SJ, Miner MD, Li C, Chaichitehrani N, O'Connor M, & Wang J. 2016. Assessment of Mud-Capped Dredge Pit Evolution Offshore Louisiana: Implications to Sand Excavation and Coastal Restoration. Paper presented at: AGU Ocean Sciences Meeting; New Orleans, LA.
- Xue Z, Wilson CA, Xu KH, et al. 2022. Sandy borrow area sedimentation-characteristics and processes within South Pelto dredge pit on Ship Shoal, Louisiana shelf, USA. *Estuar Coast.* 1-19.



### **Department of the Interior (DOI)**

The Department of the Interior protects and manages the Nation's natural resources and cultural heritage; provides scientific and other information about those resources; and honors the Nation's trust responsibilities or special commitments to American Indians, Alaska Natives, and affiliated island communities.



### **Bureau of Ocean Energy Management (BOEM)**

The mission of the Bureau of Ocean Energy Management is to manage development of U.S. Outer Continental Shelf energy and mineral resources in an environmentally and economically responsible way.

### **BOEM Environmental Studies Program**

The mission of the Environmental Studies Program is to provide the information needed to predict, assess, and manage impacts from offshore energy and marine mineral exploration, development, and production activities on human, marine, and coastal environments. The proposal, selection, research, review, collaboration, production, and dissemination of each of BOEM's Environmental Studies follows the DOI Code of Scientific and Scholarly Conduct, in support of a culture of scientific and professional integrity, as set out in the DOI Departmental Manual (305 DM 3).